

Supplementary Information for

Disruption of KMT2D perturbs germinal center B cell development and promotes lymphomagenesis

Jiyuan Zhang¹, David Dominguez-Sola^{1,2,3}, Shafinaz Hussein^{1,10}, Ji-Eun Lee⁴, Antony B. Holmes¹, Mukesh Bansal⁵, Sofija Vlasevska¹, Tongwei Mo¹, Hongyan Tang¹, Katia Basso^{1,6}, Kai Ge⁴, Riccardo Dalla-Favera^{1,6–9} and Laura Pasqualucci^{1,6,9*}

¹ Institute for Cancer Genetics, Columbia University, New York, NY, USA

² Department of Oncological Sciences, Icahn School of Medicine at Mount Sinai, New York, NY, USA

³ Department of Pathology, Icahn School of Medicine at Mount Sinai, New York, NY, USA

⁴ Laboratory of Endocrinology and Receptor Biology, National Institute of Diabetes and Digestive and Kidney Diseases, National Institutes of Health, Bethesda, MD, USA

⁵ Department of Systems Biology, Columbia University, New York, NY, USA

⁶ Department of Pathology and Cell Biology, Columbia University, New York, NY, USA

⁷ Department of Genetics & Development, Columbia University, New York, NY, USA

⁸ Department of Microbiology & Immunology, Columbia University, New York, NY, USA

⁹ Herbert Irving Comprehensive Cancer Center, Columbia University, New York, NY, USA

¹⁰ Current address: Department of Pathology and Laboratory Medicine, North Shore LIJ Health System, Staten Island University Hospital, New York, NY, USA

* Corresponding Author: Laura Pasqualucci (lp171@columbia.edu)

SUPPLEMENTARY NOTES

ChIP-seq analysis of KMT2D binding in human GC B cells

To begin to define the biochemical functions of KMT2D in the GC, we examined its genome-wide binding pattern in two independently purified pools of human GC B cells ($CD77^+$) by ChIP-seq analysis using a specific, experimentally validated antibody (see **Supplementary Fig. 2d,e**). The same cells were investigated for mapping of H3K4me1, H3K4me3 and H3K27Ac in order to functionally characterize the bound chromatin. This analysis identified 4,153 genomic regions that were significantly bound by KMT2D in both biological replicates ($P < 10^{-5}$), and comprised proximal promoter regions ($-2/+1$ Kb from TSS; $n = 2,409$, 58%) and more distal regions (either intragenic: $n = 789$, 19%; or intergenic: $n = 955$, 23%), representing putative enhancers (**Supplementary Fig. 10b**). As expected, KMT2D-bound regions were enriched in active epigenetic marks, consistent with the notion that this enzyme is responsible for implementing active chromatin modifications¹; particularly, we found significant overlap between KMT2D occupancy and H3K4me3 at transcription start sites (TSS), indicative of active promoters ($n = 2,286$ peaks, 55%), and between KMT2D and both H3K4me1 and H3K27Ac at TSS distal sites (>5 kb), a chromatin property of active enhancers ($n = 1,218$ peaks, 29%)^{2,3}. Notably, 515 of the “active” peaks mapped to 349 genomic regions that were predicted by the ROSE algorithm to represent GC super-enhancers (see Methods)⁴, and were also recently identified as super-enhancers in DLBCL cells⁵ (**Supplementary Fig. 10c**). The data described above indicate that, analogous to its role in other organisms and tissue types, KMT2D is a major mono-methyltransferase at enhancers even in GC B cells; additionally, a substantial part of the KMT2D-modulated program seems to involve its activity at promoter regions.

SUPPLEMENTARY FIGURE LEGENDS

Supplementary Fig. 1. KMT2D mRNA expression in mature B cell subsets. (a) Expression levels of KMT2D and KMT2C mRNA in naive, GC and memory B cells purified from reactive human tonsils, measured by RNA-seq ($n = 3$ donors each, representing 3 biological replicates; mean \pm SD). Data were normalized to the total number of mapped reads in each sample and to the transcript size, and are expressed as reads per kilobase per million mapped reads (RPKM). ** $P < 0.01$, Student's *t*-test. (b) Expression levels of KMT2D and KMT2C in GC dark zone (DZ) and light zone (LZ) B cells sorted from reactive human tonsils or from the spleen of immunized mice, and analyzed by gene expression profiling using Affymetrix HG U133_plus 2 (human) or MG_430_2.0 (mouse) arrays (Accession No: GSE38697 and GSE38696, respectively). Data (RMA-normalized) are expressed as linear absolute values, and the probe ID is provided for each transcript ($n = 4$ donors/subset, representing biological replicates; mean \pm SD). * $P < 0.05$, Student's *t*-test. Only statistically significant differences are indicated in the figure.

Supplementary Fig. 2. Validation of anti-KMT2D antibodies. (a) Schematic representation of the KMT2D protein (NP_003473.3), with its known functional domains. The epitopes recognized by the anti-KMT2D-S (green), KMT2D-1185 (red), KMT2D-1184 (black) and KDM2D-1183 (purple) antibodies are approximately positioned above the cartoon, with their amino acid coordinates (GenBank accession number NP_003473.3). (b) IHC analysis of KMT2D expression using the anti-KMT2D-S antibody documents the presence of nuclear-positive cells in a cell line (OCI-LY8) carrying wild-type *KMT2D* alleles and expressing the full-

length KMT2D protein by immunoblot analysis, but not in the OCI-LY18 cell line, which carries biallelic frameshift (fs) mutations abrogating the epitope, and does not express an intact KMT2D protein by immunoblot analysis (see also **Fig. 1b**). The right panel shows a primary tumor sample harboring two truncated *KMT2D* alleles, one of which partially retains the exons encoding for the specific epitope, and can thus be recognized by this antibody. Scale bar, 30 μ m. Data represent one experiment out of three that produced analogous results. **(c)** Immunoblot analysis using the anti-KMT2D-1184 antibody in whole cell extracts from HEK 293T cells transfected with vectors expressing a wild-type (WT) *KMT2D* allele or the E4712* truncated *KMT2D* allele found in SUDHL6. The endogenous KMT2D protein is not detected because of the very short exposure. One of two independent experiments that gave analogous results. **(d)** Immunoblot analysis of immunoprecipitates obtained from the Val cell line (*KMT2D* WT) using nine different anti-KMT2D antibodies (see **Supplementary Table 7**), and a rabbit IgG isotype control antibody. The KMT2D-S antibody, which showed an optimal signal to noise ratio, was selected for further validation and ChIP-seq experiments. Asterisks indicate non-specific background signal that was also detected by the isotype control antibody. Data are representative of one experiment. **(e)** Immunoblot analysis of KMT2D, RBBP5 and α -tubulin (control for input) in *KMT2D*-WT and *KMT2D*-truncated DLBCL cell lines, before (input) and after immunoprecipitation with the anti-KMT2D-S antibody (or an IgG isotype control). The antibody is able to co-immunoprecipitate the core COMPASS subunit RBBP5^{6,7} only in *KMT2D*-WT cells, documenting the lack of cross-reactivity with KMT2C. For brevity, the anti-KMT2D-1185 antibody, which was then used in all immunoblot analyses of human samples, is called KMT2D in the main manuscript. **(f)** Mutation features and predicted molecular weight of the truncated proteins in *KMT2D*-mutated DLBCL cell lines. A and B denote the two alleles. **(g)** Immunoblot

analysis of the cell lines shown in panel **f**, using the anti-KMT2D-1184 antibody. Arrow indicates the expected molecular weight of the intact KMT2D protein (593 kDa), while asterisks denote the area where the truncated proteins are expected to migrate (red if the epitope recognized by the antibody is retained, green if the epitope is lost, and thus cannot be detected). The analysis failed to reveal any signal corresponding to the expected truncated proteins, even upon MG132 treatment and immunoprecipitation (not shown), suggesting that mechanisms other than proteosomal-mediated degradation are responsible for their lack of expression. Data represent one experiment out of three that gave analogous results.

Supplementary Fig. 3. Distribution pattern of *KMT2D* mutations in *de novo* DLBCL and tFL. **(a)** Distribution of missense mutations along the KMT2D protein, with its known functional domains (PHD, plant homeodomain; HMG, High Mobility Group; FYRN, FY-rich, N-terminal; FYRC, FY-rich, C-terminal; SET, Su(var)3-9, Enhancer-of-zeste, Trithorax). **(b)** Overall percentage of cases carrying *KMT2D* non-silent mutations in tFL and DLBCL. Data integrate published studies by our and other groups, as indicated; nd, not determined (no information was available in this study to unequivocally calculate the fraction of cases carrying missense vs truncating mutations; thus, the overall percentage of primary DLBCL biopsies harboring missense mutations in the three datasets may represent an underestimate).

Supplementary Fig. 4. Missense mutations do not affect KMT2D protein stability. **(a)** Features of the *KMT2D* missense mutations tested *in vitro*. **(b)** Immunoblot (top) and qRT-PCR (bottom) analysis of exogenous KMT2D expression in HEK 293T cells transfected with equimolar amounts of vectors expressing HA-tagged wild-type or mutant *KMT2D* alleles. Actin

controls for loading. qRT-PCR results are expressed as relative fold changes vs wild-type KMT2D, which was arbitrarily set as 1 (dotted red line) (mean \pm SD, one of two independent experiments performed in triplicate, which gave analogous results). Note that the S5404F mutant (in blue) showed significantly lower levels compared to the wild-type KMT2D protein in multiple independent experiments ($P = 0.01$, Student's *t*-test), despite comparable mRNA levels, consistent with protein instability. This mutant was therefore not included in the histone methyltransferase assays shown in **Fig. 2c,d**.

Supplementary Fig. 5. Analysis of bone marrow (BM) and peripheral B cell subsets in unimmunized *Kmt2d*^{fl/fl}*CD19-Cre* mice. (a) Representative flow cytometric analysis of BM B cell subsets in 12 to 16-weeks old *Kmt2d*^{+/+}*CD19-Cre*, *Kmt2d*^{fl/+}*CD19-Cre* and *Kmt2d*^{fl/fl}*CD19-Cre* mice left unimmunized. Numbers indicate the percentage of cells in each gate, relative to total BM nucleated cells (top panel) or to the population in the gate indicated above the plot (bottom panel). (b) Quantification of 3 mice/genotype (mean \pm SD; data are representative of one experiment). Pro and pre B cells are defined as CD93^{hi}B220^{int}IgM⁻, immature B cells are CD93^{hi}B220^{int}IgM⁺, and mature recirculating B cells are B220^{hi}CD93^{low}. (c) Representative flow cytometric analysis of splenic B220⁺ (top), follicular (FO: B220⁺CD21^{int}CD23^{hi}) and marginal zone (MZ: B220⁺CD21^{hi}CD23^{low}) B cells (bottom) in the same animals. Numbers indicate the percentage of cells in each gate, relative to total erythrocyte-depleted splenocytes (top) or to B220⁺ cells (bottom). (d) Quantification of 3 mice/genotype (mean \pm SD; data are representative of one experiment). * $P < 0.05$, one-way ANOVA. Only statistically significant differences are highlighted in the figure.

Supplementary Fig. 6. *Kmt2d*^{fl/fl}*CD19-Cre* mice show reduced numbers of follicular B cells.

(a) Representative flow cytometric analysis of BM B cell subsets in 12–16 weeks old *Kmt2d*^{+/+}*CD19-Cre*, *Kmt2d*^{fl/+}*CD19-Cre* and *Kmt2d*^{fl/fl}*CD19-Cre* mice, analyzed 10 days after SRBC immunization. Numbers indicate the percentage of BM nucleated cells in each gate, relative to total BM nucleated cells (top panel) or to the population in the gate indicated above the plot. (b) Percentage (left) and absolute number (right) of pro/pre ($\text{CD93}^{\text{hi}}\text{B220}^{\text{int}}\text{IgM}^-$), immature ($\text{CD93}^{\text{hi}}\text{B220}^{\text{int}}\text{IgM}^+$) and mature recirculating B cells ($\text{B220}^{\text{hi}}\text{CD93}^{\text{low}}$) in the BM of the indicated mice (mean \pm SD; $n = 4$ *Kmt2d*^{+/+}*CD19-Cre*, 4 *Kmt2d*^{fl/+}*CD19-Cre* and 3 *Kmt2d*^{fl/fl}*CD19-Cre* mice; percentages are from one of four independent experiments, which gave analogous results on a total of 12 mice; absolute numbers are from one of two independent experiments). * $P < 0.05$, one-way ANOVA. Five-color staining for surface expression of B220, IgM, IgD, CD19 and CD25 in the same animals confirmed the significant reduction in mature recirculating B cells ($\text{B220}^+\text{IgD}^{\text{hi}}$) and did not show statistically significant differences in the number of prepro- ($\text{B220}^+\text{IgD}^{\text{lo}}\text{CD19}^{\text{lo}}$), pro- ($\text{B220}^+\text{IgD}^{\text{lo}}\text{CD19}^{\text{hi}}\text{IgM}^{\text{lo}}\text{CD25}^-$), pre ($\text{B220}^+\text{IgD}^{\text{lo}}\text{CD19}^{\text{hi}}\text{IgM}^{\text{lo}}\text{CD25}^+$) and immature ($\text{B220}^+\text{IgD}^{\text{lo}}\text{CD19}^{\text{hi}}\text{IgM}^{\text{hi}}\text{CD25}^-$) B cells (not shown). (c) Representative flow cytometric analysis of splenic cell suspensions from 12–16 weeks old *Kmt2d*^{+/+}*CD19-Cre*, *Kmt2d*^{fl/+}*CD19-Cre* and *Kmt2d*^{fl/fl}*CD19-Cre* mice, analyzed 10 days after SRBC immunization. Splenocytes were stained with anti-B220-PerCP, anti-CD93 (AA4.1)-PE.Cy7, anti-sIgM-APC, anti-IgD-VioGreen, anti-CD23-PE and anti-CD21-FITC. B cells are identified as B220^+ cells in the live lymphocyte gate (top panels). T1, T2 and T3 B cells are identified as $\text{IgM}^{\text{hi}}\text{CD23}^-$ (T1), $\text{IgM}^{\text{hi}}\text{CD23}^+$ (T2), and $\text{IgM}^{\text{low}}\text{CD23}^+$ (T3) cells in the $\text{B220}^+\text{CD93}^+$ population (middle panels). The bottom panel shows representative dot plots for FO ($\text{B220}^+\text{CD21}^{\text{int}}\text{CD23}^+$) and MZ ($\text{B220}^+\text{CD21}^{\text{hi}}\text{CD23}^{\text{low}}$) B cells. Numbers indicate the

percentage of cells in the gate, relative to total erythrocyte-depleted splenocytes or to the population indicated above the plot. **(d)** Absolute number of peripheral B cell subsets in the spleen (left) and mesenteric lymph nodes (MSLN, right) of mice from the indicated genotypes, analyzed 10 days after SRBC immunization (mean \pm SD; $n = 4$ $Kmt2d^{+/+}CD19-Cre$, 4 $Kmt2d^{fl/fl}CD19-Cre$ and 3 $Kmt2d^{fl/fl}CD19-Cre$; data for FO and MZ B cells represent one out of four independent experiments that gave analogous results in a total of 12 animals/genotype; data for transitional B cells and MSLN represent one experiment out of two that gave analogous results on a total of 5-7 animals/genotype). * $P < 0.05$, ** $P < 0.01$, one-way ANOVA. Only statistically significant differences are highlighted in the figure. Although $Kmt2d^{fl/fl}CD19-Cre$ mice showed a trend towards reduced numbers of T2 and T3 cells, these differences did not reach statistical significance.

Supplementary Fig. 7. $Kmt2d^{fl/fl}C\gamma I-Cre$ mice display normal GC development. **(a)** Quantitative RT-PCR analysis of Kmt2d expression in GC B cells from 8–12 weeks old $Kmt2d^{+/+}C\gamma I-Cre$, $Kmt2d^{fl/fl}C\gamma I-Cre$ and $Kmt2d^{fl/fl}C\gamma I-Cre$ littermates. Results are expressed as relative fold change vs the mean of $Kmt2d^{+/+}C\gamma I-Cre$ samples, which was arbitrarily set at 1 ($n = 3$ mice/genotype, mean \pm SD, one experiment performed in triplicate). * $P < 0.05$, ** $P < 0.01$, one-way ANOVA. **(b)** Immunoblot analysis of Kmt2d and H3K4 methylation marks in sorted GC B cells. Total H3 and actin serve as loading control in the chromatin extracts and whole cell extracts, respectively. Each sample corresponds to two pooled mice, owing to the low number of GC cells that can be sorted from a single mouse spleen. Quantification of signal intensity for the three histone marks, after normalization for total H3, is provided in the right panel. **(c)** Representative flow cytometric analysis of splenic B220 $^+$ cells from 12 weeks old $Kmt2d^{+/+}C\gamma I-$

Cre, *Kmt2d*^{fl/fl}*CγI-Cre* and *Kmt2d*^{fl/fl}*CγI-Cre* mice analyzed at day 10 after SRBC immunization. GC B cells are identified as CD95⁺PNA^{hi} cells, and numbers in each panel indicate the percentage in the gate. (d) Percentage of GC B cells in mice from the indicated genotypes, analyzed at 3 months ($n = 7$ *Kmt2d*^{+/+}*CγI-Cre*, 7 *Kmt2d*^{fl/fl}*CγI-Cre* and 6 *Kmt2d*^{fl/fl}*CγI-Cre*; data pooled from two independent experiments) and 6 months of age ($n = 5$ *Kmt2d*^{+/+}*CγI-Cre*, 5 *Kmt2d*^{fl/fl}*CγI-Cre* and 4 *Kmt2d*^{fl/fl}*CγI-Cre*; data represent one experiment), 10 days after SRBC immunization. (e) Quantification of mean GC size, GC number and total GC area (per spleen section) in the same animals, analyzed at 3 and 6 months of age, 10 days after SRBC immunization. Analysis was performed on FFPE sections stained for the GC marker Bcl6, using the ImageJ software (<http://imagej.nih.gov/ij/>), and values represent the mean \pm SD, after normalization to the total spleen area, with average levels from controls set at 1. ($n = 5$ *Kmt2d*^{+/+}*CγI-Cre*, 4 *Kmt2d*^{fl/fl}*CγI-Cre*, and 3 *Kmt2d*^{fl/fl}*CγI-Cre* at 3 months of age; $n = 5$ *Kmt2d*^{+/+}*CγI-Cre*, 5 *Kmt2d*^{fl/fl}*CγI-Cre*, and 4 *Kmt2d*^{fl/fl}*CγI-Cre* at 6 months of age). (f) Percentage of plasma cells (left) and surface IgG1⁺ cells (right) in the same animals shown in d (mean \pm SD). (g) Total IgM and IgG serum levels in 3-month old SRBC-immunized animals, as determined by ELISA prior to (d0, $n = 3$ mice/genotype) and 10 days after immunization (d10, $n = 6$ mice/genotype). In all panels, *ns* denotes not significant, one-way ANOVA.

Supplementary Fig. 8. *Kmt2d*^{fl/fl}*CD19-Cre* mice show increased surface IgG1⁺ cells. (a) Representative flow cytometric analysis of splenic lymphocytes from 8–12 weeks old SRBC-immunized *Kmt2d*^{+/+}*CD19-Cre*, *Kmt2d*^{fl/+}*CD19-Cre* and *Kmt2d*^{fl/fl}*CD19-Cre* littermates, stained for B220 and surface IgG1; numbers indicate the percentage of IgG1 switched B cells (gated population) in the total lymphocyte population (left). The quantification (percentage and absolute

numbers) of animals analyzed at 3 ($n = 8/\text{genotype}$) and 6 ($n = 4\text{--}5/\text{genotype}$) months of age is shown on the right panel, where each symbol represents one animal. *: $P < 0.05$, one-way ANOVA. **(b)** Representative flow cytometric analysis of splenocytes from $Kmt2d^{+/+}CD19\text{-}Cre$, $Kmt2d^{fl/+}CD19\text{-}Cre$ and $Kmt2d^{fl/fl}CD19\text{-}Cre$ littermates, analyzed at 3 months of age, 10 days after SRBC immunization. Percentages indicate the proportion of $\text{B220}^-\text{CD138}^{\text{hi}}$ plasma cells in the gate. The quantification (percentage and absolute numbers) of animals analyzed at 3 ($n = 8/\text{genotype}$) and 6 ($n = 4\text{--}5/\text{genotype}$) months of age is shown on the right. *: $P < 0.05$, one-way ANOVA. **(c)** Total IgM (top) and IgG1 (bottom) serum levels in 3 months old, SRBC-immunized animals ($n = 5/\text{genotype}$), as compared to unimmunized mice (d0) ($n = 3/\text{genotype}$). *: $P < 0.05$, one-way ANOVA. In all panels, *ns* denotes not significant, one-way ANOVA.

Supplementary Fig. 9. Deletion of *Kmt2d* early in B cell development leads to increased GC formation and reduced serum levels after NP-KLH immunization. **(a)** Representative flow cytometric analysis of GC B cells in splenic B220^+ cells from 8–12 weeks old $Kmt2d^{+/+}CD19\text{-}Cre$, $Kmt2d^{fl/+}CD19\text{-}Cre$ and $Kmt2d^{fl/fl}CD19\text{-}Cre$ mice analyzed at day 0, 12 and 28 after immunization with the NP-KLH hapten. GC B cells are identified as $\text{CD95}^+\text{PNA}^{\text{hi}}$ cells, and numbers in each panel indicate the percentage in the gate. **(b)** Quantification of data shown in **a** ($n = 3$ mice/genotype at d0, 5–7 mice/genotype at d12, and 3–4 mice/genotype at d28). * $P < 0.05$, ** $P < 0.01$, *ns* = not significant, one-way ANOVA. **(c)** Representative FACS analysis of DZ and LZ fractions in splenic $\text{B220}^+\text{CD95}^+\text{PNA}^+$ GC B cells from 8–12 weeks old mice, analyzed at day 12 after NP-KLH immunization. DZ cells are identified as $\text{CXCR4}^{\text{hi}}\text{CD86}^{\text{lo}}$, while LZ cells are $\text{CXCR4}^{\text{lo}}\text{CD86}^{\text{hi}}$ (ref. 8,9). Numbers in each panel indicate the percentage in the gate. **(d)** Relative ratio of DZ/LZ B cells in the same mice ($n = 7$ $Kmt2d^{+/+}CD19\text{-}Cre$, 7

Kmt2d^{f/+}*CD19-Cre*, and 5 *Kmt2d*^{fl/fl}*CD19-Cre*). *ns* = not significant, one-way ANOVA. (e) High affinity (NP₅) and low affinity (NP₂₅) IgG1 antibody titers in the serum of 8–12 weeks old *Kmt2d*^{+/+}*CD19-Cre*, *Kmt2d*^{f/+}*CD19-Cre* and *Kmt2d*^{fl/fl}*CD19-Cre* mice, measured prior to (d0) and 12 or 28 days after immunization with NP-KLH. The NP₅/NP₂₅ ratio and the amount of high affinity (NP₂₅) IgM antibody titers are also shown (*n* = 3 mice/genotype, representative of one experiment) * *P* < 0.05, ** *P* < 0.01, *ns* = not significant, one-way ANOVA. (f) Percentage of V186.2 rearrangements carrying the hotspot W33L mutation in GC B cells sorted from mice of the indicated genotypes 12 days after NP-KLH immunization. Data are pooled from two independent experiments (*n* = 7 *Kmt2d*^{+/+}*CD19-Cre*, 7 *Kmt2d*^{f/+}*CD19-Cre* and 5 *Kmt2d*^{fl/fl}*CD19-Cre* littermates). ** *P* < 0.01, Fisher's exact test. (g) Proportion of clones harboring the indicated numbers of unique mutations in the animals shown in panel b. The total number of unique sequences analyzed is shown in the center of the pie, and the total number of mice is given in brackets. (h) Overall mutation frequency in the rearranged immunoglobulin heavy-chain V186.2 region of the same animals. *ns* = not significant, one-way ANOVA.

Supplementary Fig. 10. Integrated GEP analysis of mouse GC B cells and ChIP-seq analysis of human GC B cells. (a) Enrichment plots of selected gene sets in the rank of genes differentially expressed between *Kmt2d*-deficient and *Kmt2d*-wild type GC B cells. Top panels, analysis performed in the *CD19-Cre* cohort; bottom panels, analysis performed in the *CγI-Cre* cohort (*n* = 3 mice/genotype). (b) Distribution pattern of KMT2D binding in human GC B cells. Pie chart shows the percentage of KMT2D peaks mapping to TSS (-2 to +1 kb; blue), intragenic regions (i.e., regions within a gene; red) and intergenic regions (i.e., regions between annotated genes; grey). The chromatin state of these regions is indicated in the doughnut chart as different

shades of the same color. **(c)** Overlap between KMT2D-bound regions (intragenic and intergenic) and predicted enhancers and super-enhancers in GC B cells. Super-enhancers were identified applying the ROSE algorithm (http://younglab.wi.mit.edu/super_enhancer_code.html)^{4,5} to H3K27Ac ChIP-seq data obtained from the same samples ($n = 2$ independent pools). **(d)** Overlap between KMT2D target genes displaying epigenetic marks of activation and genes downregulated in *Kmt2d*-deficient vs *Kmt2d*-proficient mouse GC B cells (Student's *t*-test, $P < 0.05$ and FC ≥ 1.2). The complete list of these genes, representing candidate *bona fide* direct targets of *Kmt2d* methyltransferase activity, is given in **Supplementary Table 3**.

Supplementary Fig. 11. *Kmt2d*^{f/f} *Cy1-Cre* B cells have normal proliferation and cell cycle profiles. **(a)** Representative cell proliferation profile of B220⁺ cells isolated from the spleen of *Kmt2d*^{+/+} *Cy1-Cre*, *Kmt2d*^{fl/+} *Cy1-Cre* and *Kmt2d*^{fl/fl} *Cy1-Cre* mice, labeled with the CellTrace Violet dye and cultured *ex vivo* in the presence of anti-CD40 and IL4. Individual peaks in the plot correspond to different numbers of cell divisions, as measured by flow cytometric analysis at day 3 after stimulation. The unstimulated parent population is indicated by the empty line. Numbers indicate the percentage of cells with more than two divisions, and the quantification of 3 samples/genotype is shown in panel **b**, where values represent the mean and error bars represent the standard deviation from the mean. Analysis by one-way ANOVA did not show significant difference between the indicated genotypes (data representative of one experiment). **(c)** Relative growth of B220⁺ splenocytes in the same experiment, measured by the CellTiter reagent. Data are given as fold changes relative to the mean value of control mice, measured at day 0 (mean \pm SD; $n = 3$ mice/genotype, acquired in triplicate). **(d)** Representative cell cycle profile of stimulated B220⁺ cells, labeled with Brdu and 7AAD and analyzed by flow cytometry

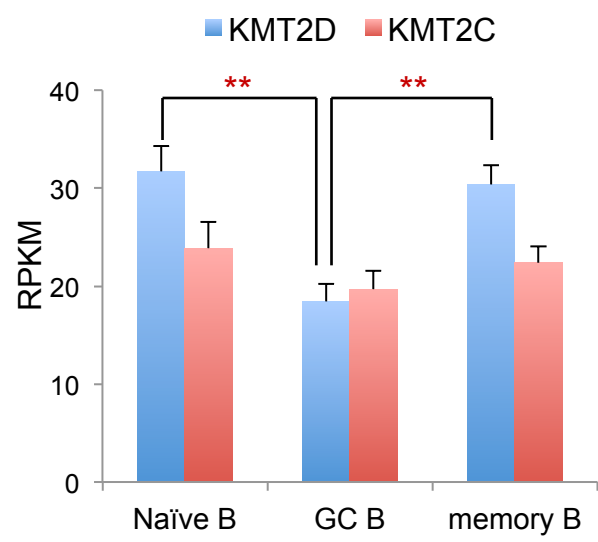
at day 3 after stimulation. Numbers indicate the percentage of cells in the gated population. (e) Quantification of panel d ($n = 3$ mice/genotype; data are representative of one experiment). (f) Immunoblot analysis of Kmt2d in whole cell lysates from $Kmt2d^{+/+}C\gamma l-Cre$, $Kmt2d^{fl/fl}C\gamma l-Cre$ and $Kmt2d^{fl/fl}C\gamma l-Cre$ B220 $^{+}$ cells, performed at day 3 of anti-CD40 + IL4 stimulation; α -tubulin, loading control ($n = 3$ mice/genotype; data are representative of one experiment).

SUPPLEMENTARY REFERENCES

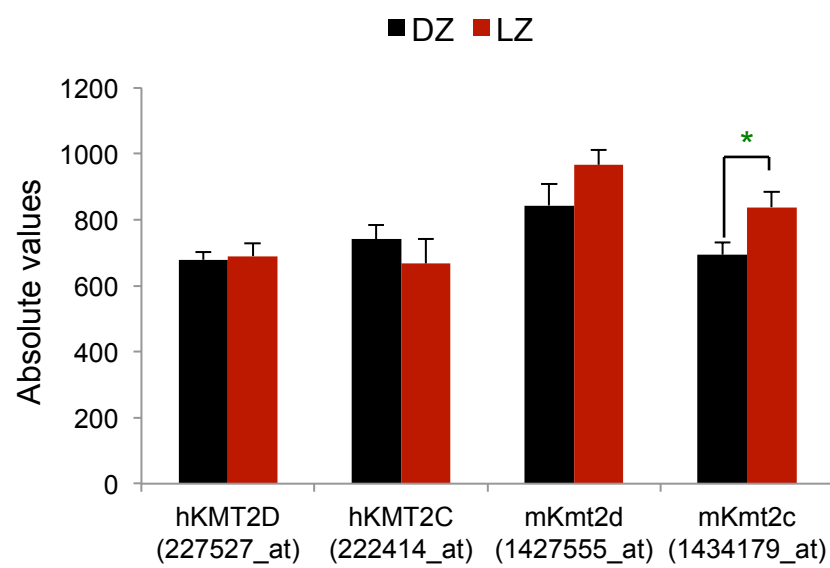
1. Shilatifard, A. The COMPASS family of histone H3K4 methylases: mechanisms of regulation in development and disease pathogenesis. *Annu Rev Biochem* **81**, 65-95 (2012).
2. Creyghton, M.P., et al. Histone H3K27ac separates active from poised enhancers and predicts developmental state. *Proc Natl Acad Sci U S A* **107**, 21931-21936 (2010).
3. Rada-Iglesias, A., et al. A unique chromatin signature uncovers early developmental enhancers in humans. *Nature* **470**, 279-283 (2011).
4. Whyte, W.A., et al. Master transcription factors and mediator establish super-enhancers at key cell identity genes. *Cell* **153**, 307-319 (2013).
5. Chapuy, B., et al. Discovery and characterization of super-enhancer-associated dependencies in diffuse large B cell lymphoma. *Cancer Cell* **24**, 777-790 (2013).
6. Cho, Y.W., et al. PTIP associates with MLL3- and MLL4-containing histone H3 lysine 4 methyltransferase complex. *J Biol Chem* **282**, 20395-20406 (2007).
7. Hu, D., et al. The MLL3/MLL4 Branches of the COMPASS Family Function as Major Histone H3K4 Monomethylases at Enhancers. *Mol Cell Biol* **33**, 4745-4754 (2013).
8. Allen, C.D., et al. Germinal center dark and light zone organization is mediated by CXCR4 and CXCR5. *Nat Immunol* **5**, 943-952 (2004).
9. Victora, G.D., et al. Germinal center dynamics revealed by multiphoton microscopy with a photoactivatable fluorescent reporter. *Cell* **143**, 592-605 (2010).

Supplementary Fig. 1

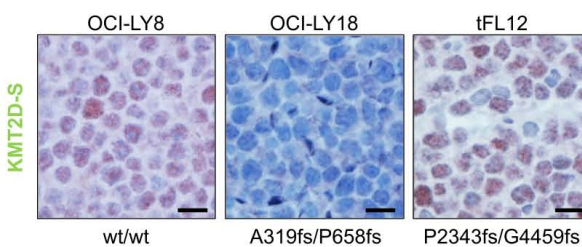
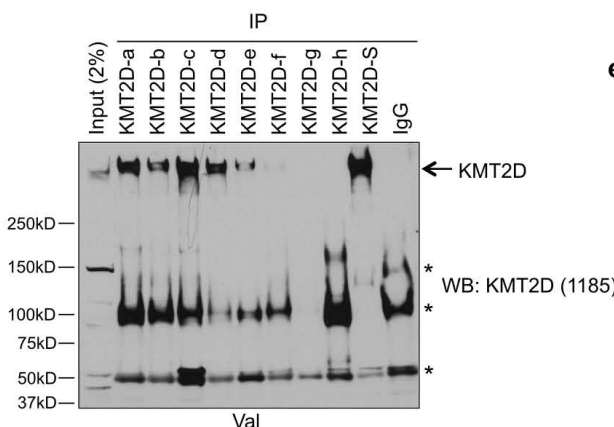
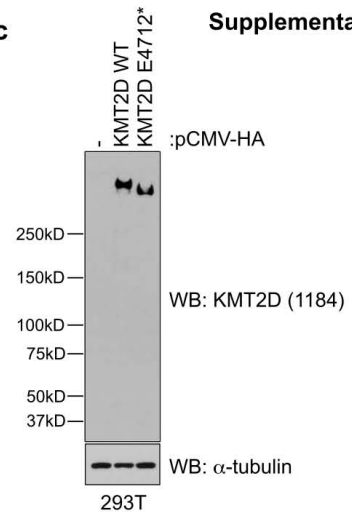
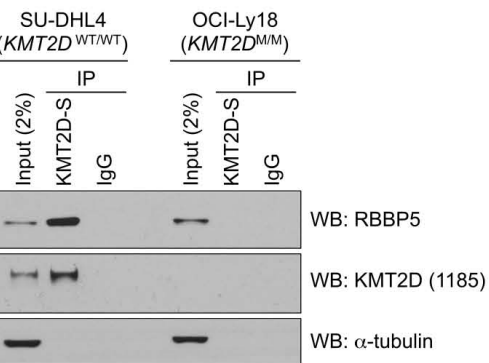
a



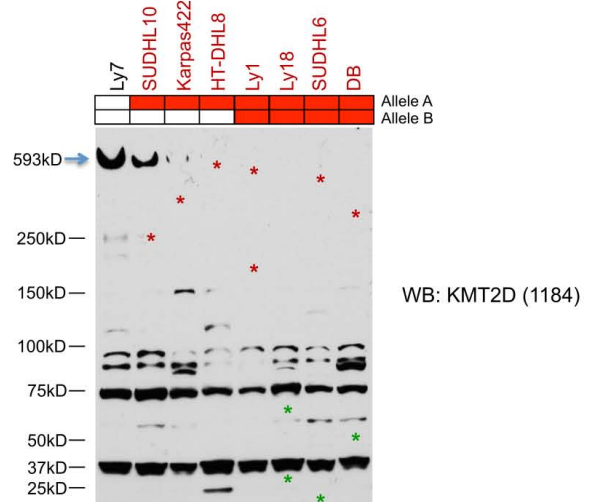
b



Supplementary Fig. 2

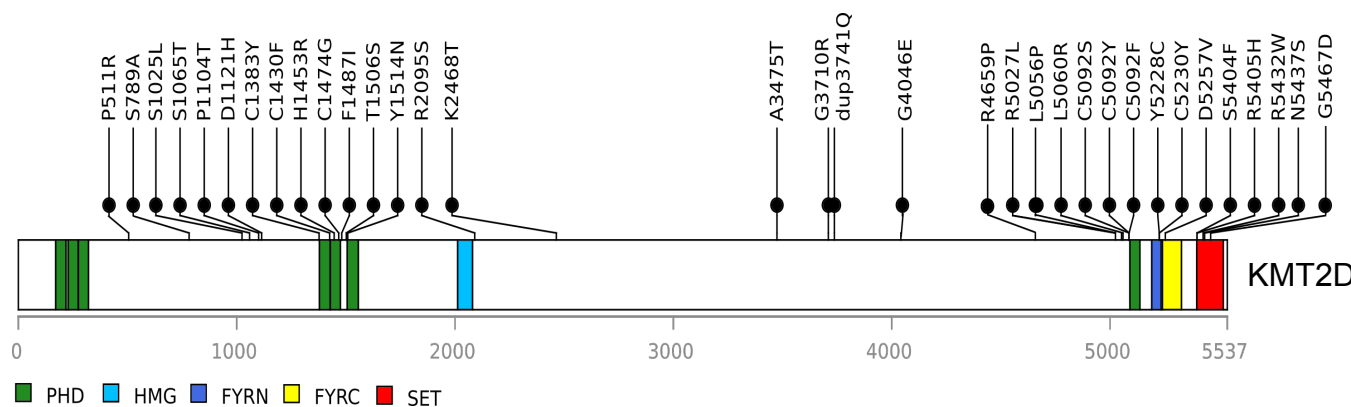
a**b****d****c****e****f**

Cell line	Allele	AA change	predicted MW (kD)
SUDHL10	A	R2410X	256.0
	B	WT	593.3
Karpas 422	A	Q3278*	346.7
	B	WT	593.3
HT-DHL8	A	G5182fs	548.8
	B	WT	593.3
Ly1	A	R1903X	202.5
	B	P4929fs	523.5
Ly18	A	P658fs	69.9
	B	A319fs	34.1
SUDHL6	A	Q211X	23.3
	B	E4712X	500.6
DB	A	Q2736*	289.7
	B	480fs	51.1

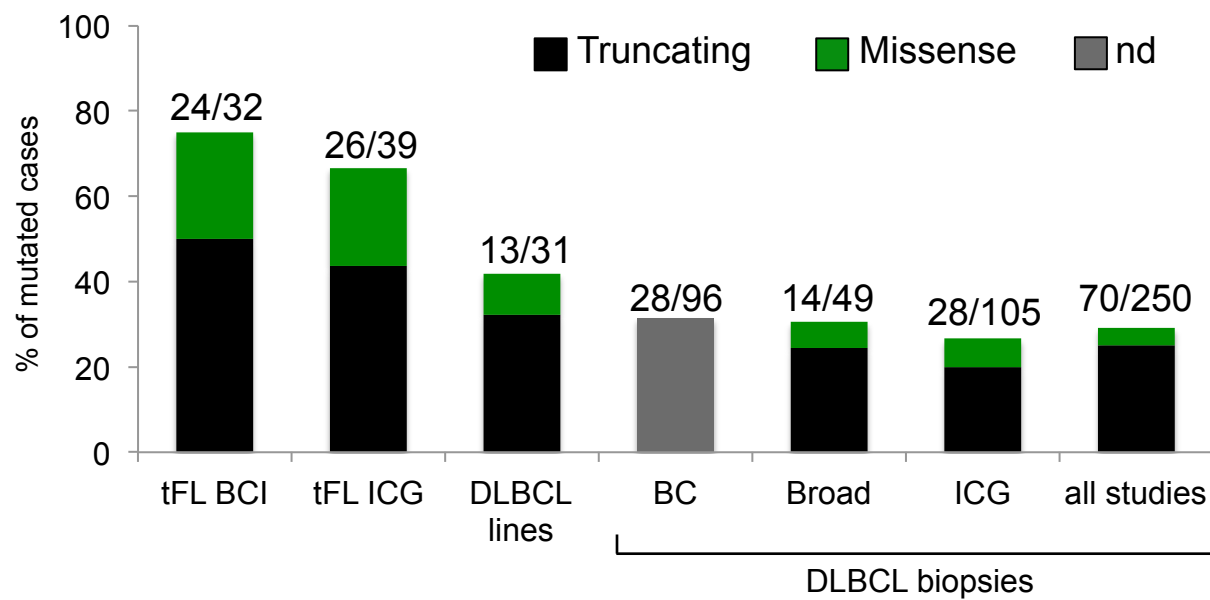
g

Supplementary Fig. 3

a



b



- **BCI**, Barts Cancer Institute, London (Okosun et al., Nature Genetics 2014 – Tables S4 and S9)
- **BC**, British Columbia Cancer Agency, Vancouver (Morin et al., Nature 2011 – Table S3)
- **Broad**, Broad Institute, Cambridge (Lohr et al., PNAS 2012)
- **ICG**, Institute for Cancer Genetics, New York (Pasqualucci et al., Nature Genetics 2011; Pasqualucci et al., Cell Rep 2014)

Supplementary Fig. 4

a

Sample ID	Diagnosis	Nucleotide Change*	AA Change*	Affected Domain^	Somatic Origin	Reference Study
2169	ABC/NC-DLBCL	T3193A	S1065T	none	undetermined	Pasqualucci et al., Nat Genetics 2011
2089	GCB-DLBCL	C3310A	P1104T	none	undetermined	Pasqualucci et al., Nat Genetics 2011
2173	ABC/NC-DLBCL	G3361C	D1121H	none	undetermined	Pasqualucci et al., Nat Genetics 2011
2171	ABC-DLBCL	C4517G	T1506S	PHD	undetermined	Pasqualucci et al., Nat Genetics 2011
7	DLBCL	C6283A	R2095S	none	somatic	Lohr et al., Proc Natl Acad Sci USA 2012**
2	DLBCL	A7403C	K2468T	none	somatic	Lohr et al., Proc Natl Acad Sci USA 2012**
2147	GCB-DLBCL	G13976C	R4659P	none	undetermined	Pasqualucci et al., Nat Genetics 2011
07-35482	GCB-DLBCL	G15080A	R5027L	none	somatic	Morin et al., Nature 2011^^
2041	NC-DLBCL	T15167C	L5056P	none	undetermined	Pasqualucci et al., Nat Genetics 2011
2027	GCB-DLBCL	T15274A	C5092S	Zinc finger, PHD type	somatic	Pasqualucci et al., Nat Genetics 2011
Toledo	GBC-DLBCL	G15275A	C5092Y	Zinc finger, PHD type	undetermined	Morin et al., Nature 2011^^
06-20952	FL	A15770T	D5257V	FYRC	somatic	Morin et al., Nature 2011^^
92-31120	FL	C16294T	R5432W	SET	somatic	Morin et al., Nature 2011^^
NU-DHL-1	GCB-DLBCL	C16211T	S5404F	SET	undetermined	Morin et al., Nature 2011^^
HT-DHL8	GCB-DLBCL	A16310G	N5437S	SET	undetermined	Pasqualucci et al., Nat Genetics 2011
12	DLBCL	G16400A	G5467D	SET	somatic	Lohr et al., Proc Natl Acad Sci USA 2012**
07-37968	GCB-DLBCL	C682G	R228G	Zinc finger, PHD type	<u>rs201994402</u>	Morin et al., Nature 2011^^
2125	GCB-DLBCL	G14395A	V4799M	none	<u>rs373731411</u>	Pasqualucci et al., Nat Genetics 2011
08-10448	FL	G15908A	R5303H	FYRC	<u>rs369156879</u>	Morin et al., Nature 2011^^

*Numbering according to GenBank accession No. NM_003482.3 (mRNA) and NP_003473.3 (protein)

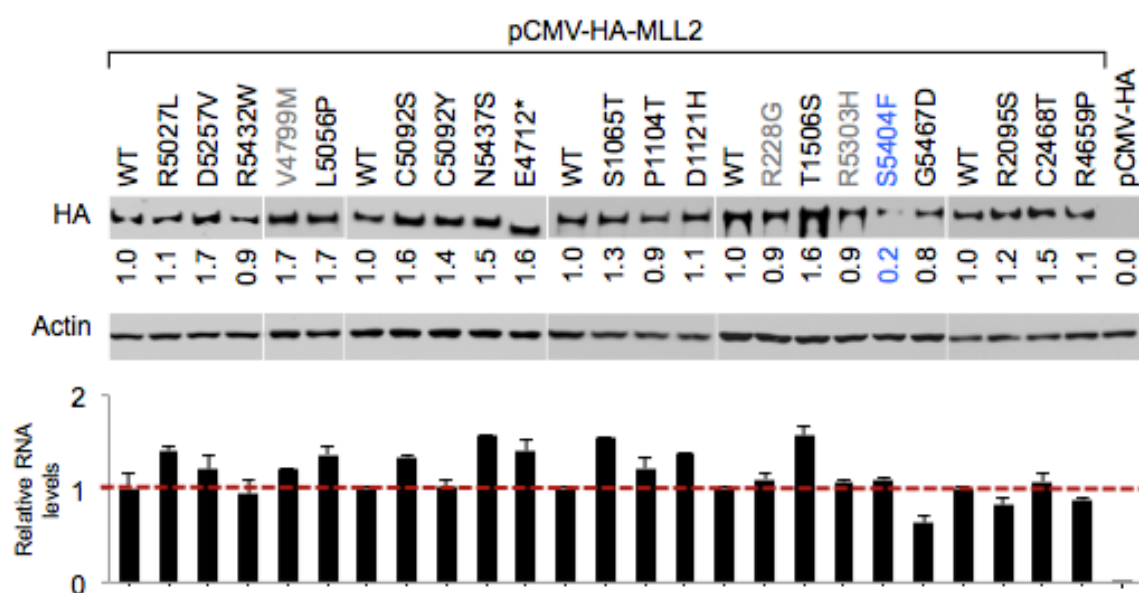
^As predicted by the SMART research tool using Swiss-Prot, SP-TrEMBL and stable Ensembl proteomes

**Data from Fig. 2

^^Data from Table S10

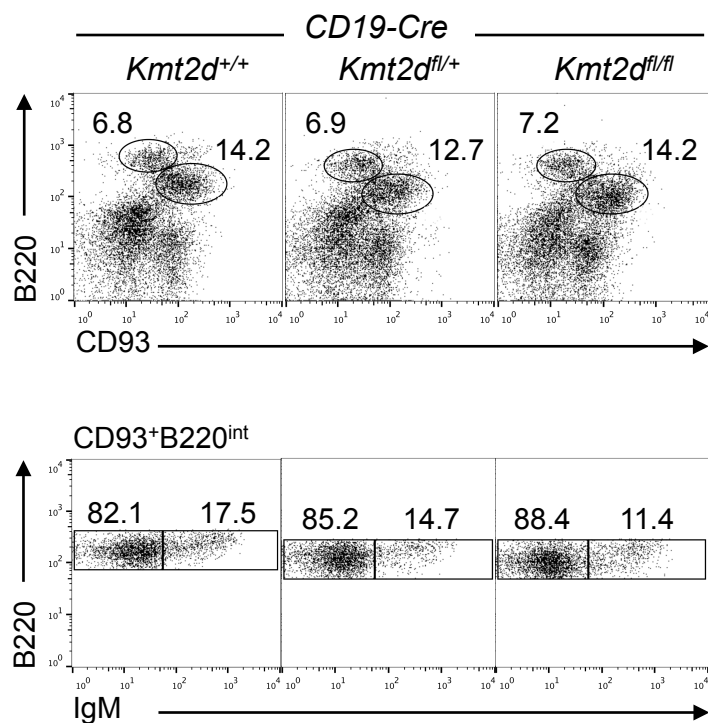
Abbreviations: DLBCL, diffuse large B cell lymphoma; ABC, activated B cell type; GCB, germinal center B cell type; NC, unclassified; FL, follicular lymphoma

b

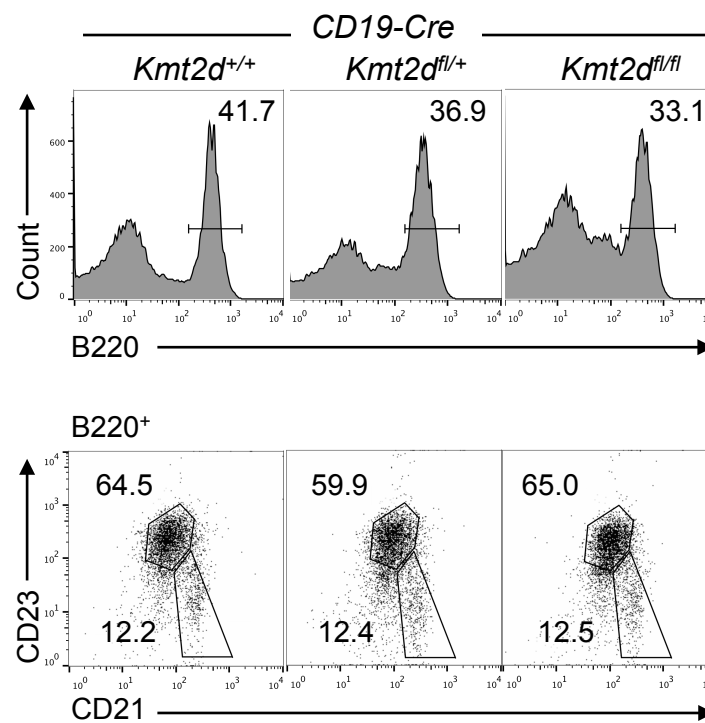


Supplementary Fig. 5

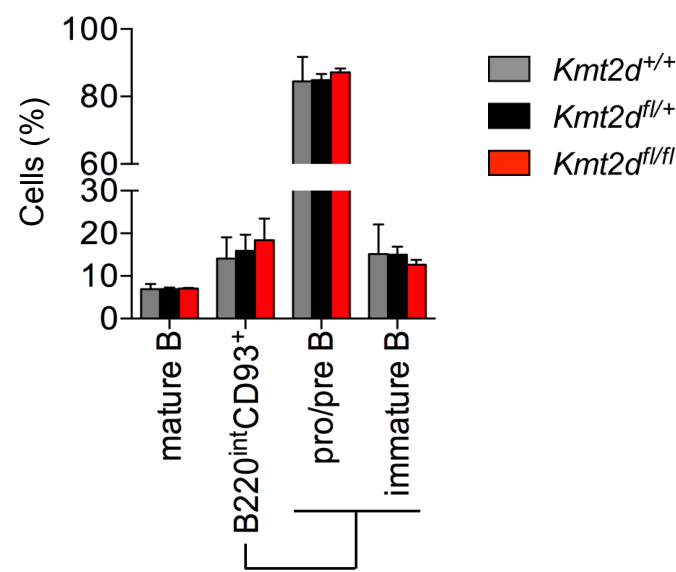
a



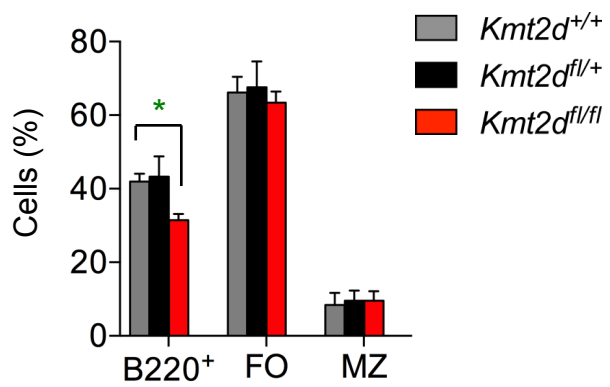
c



b

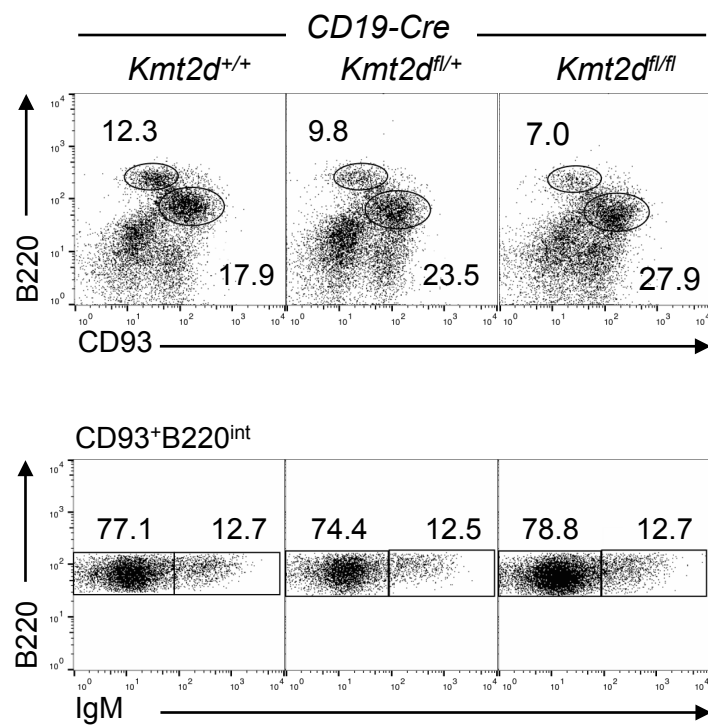


d

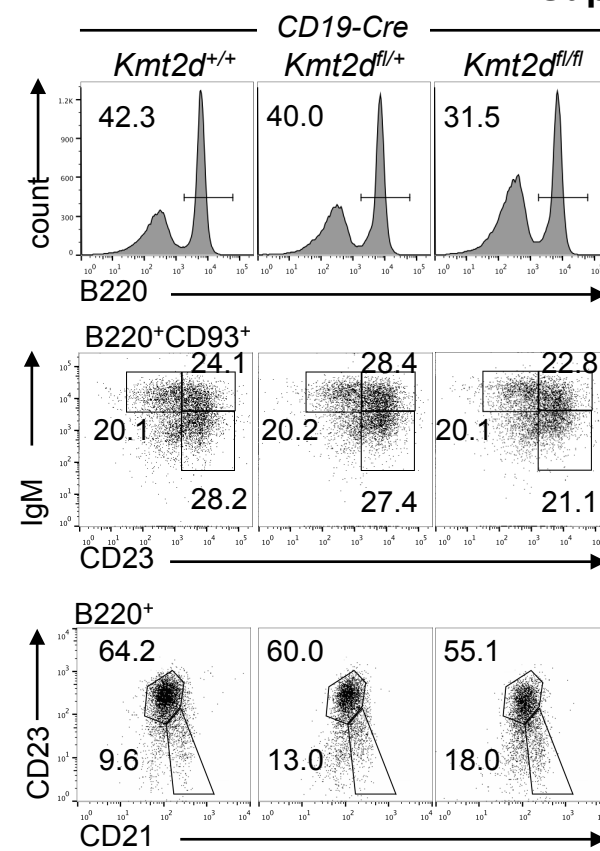


Supplementary Fig. 6

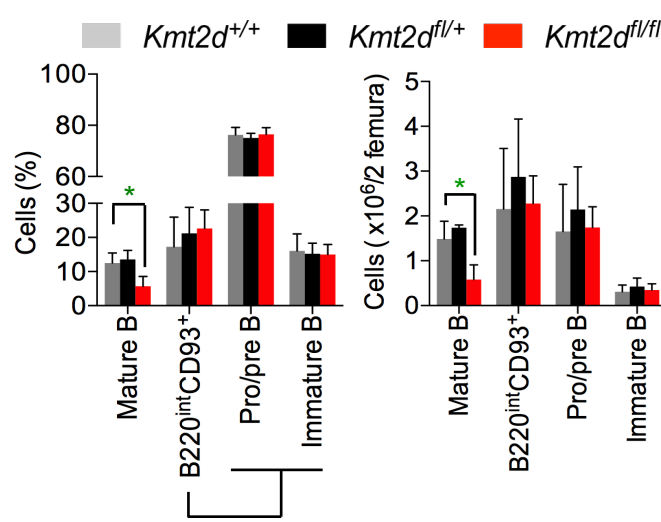
a



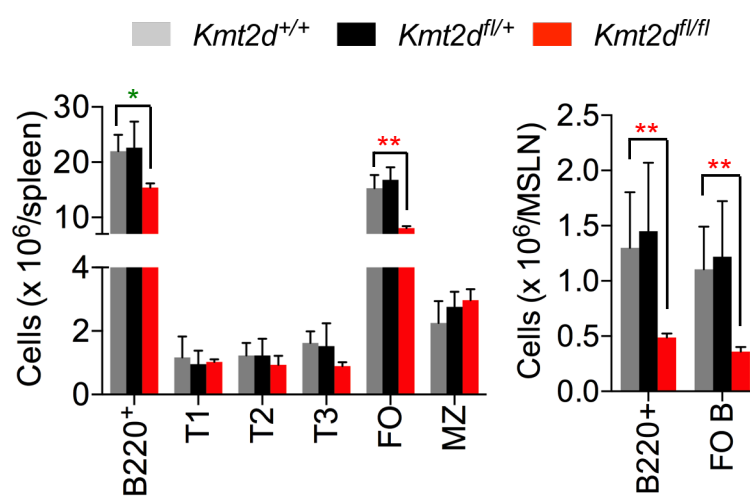
c



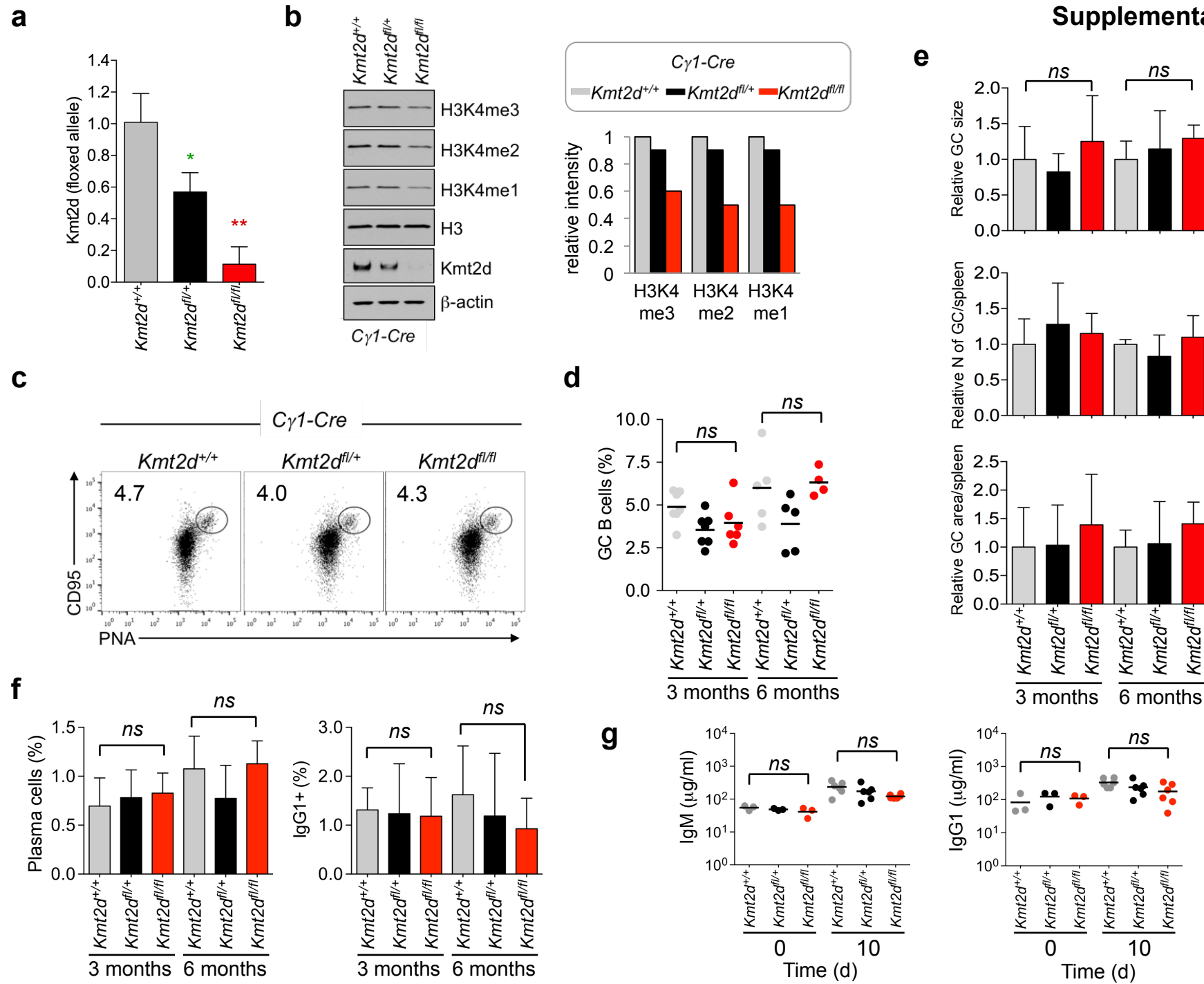
b



d

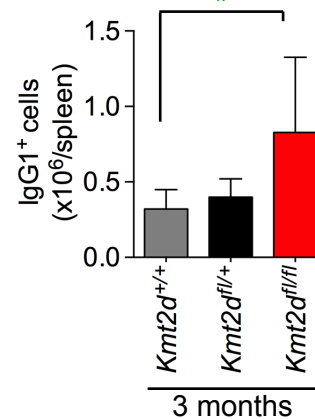
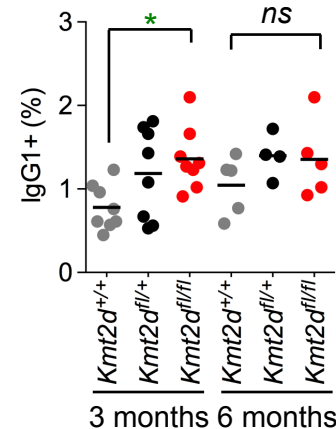
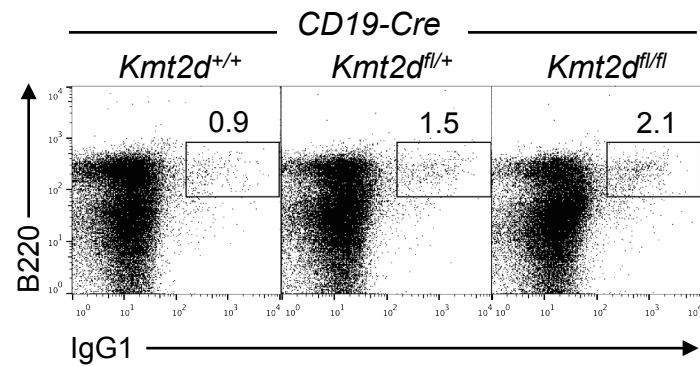


Supplementary Fig. 7

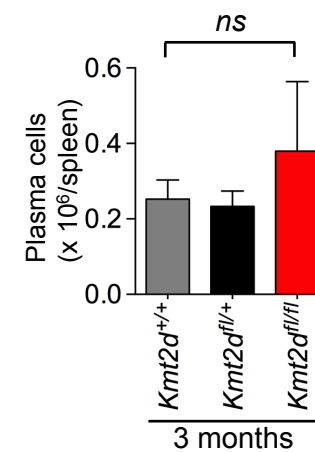
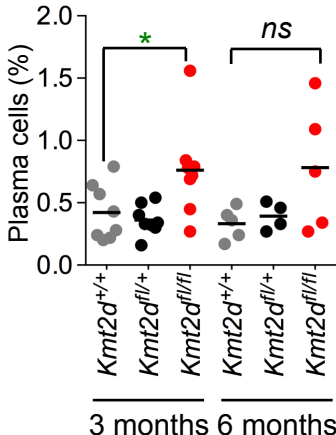
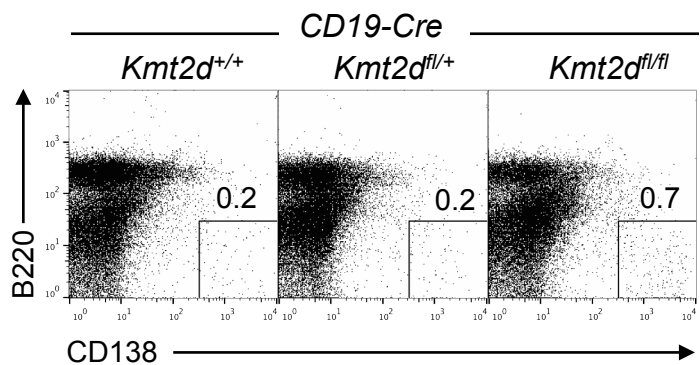


Supplementary Fig. 8

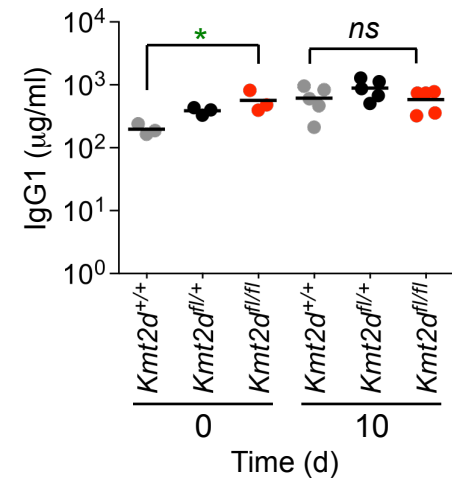
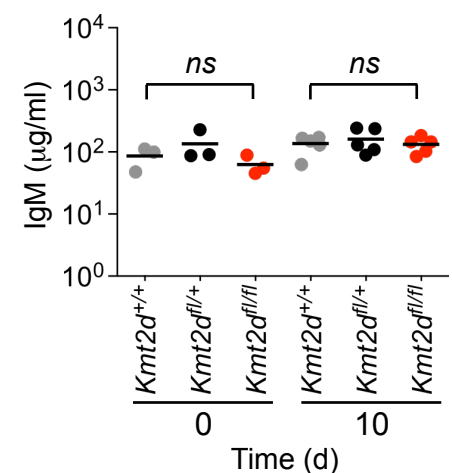
a

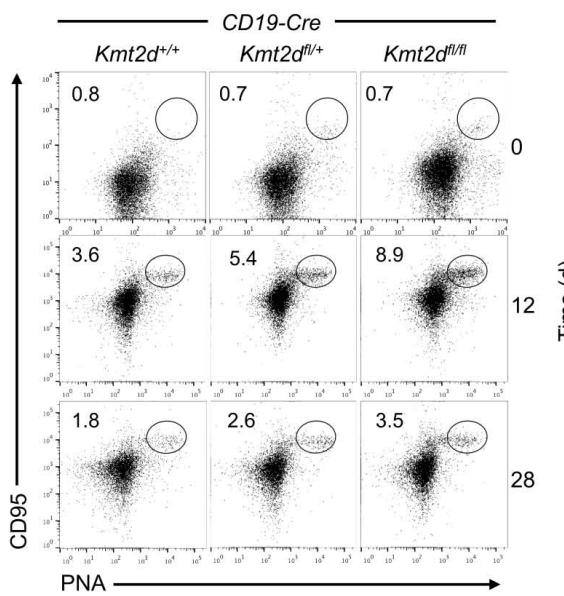
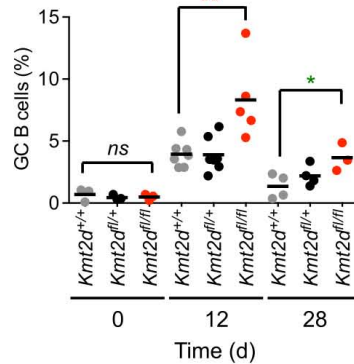
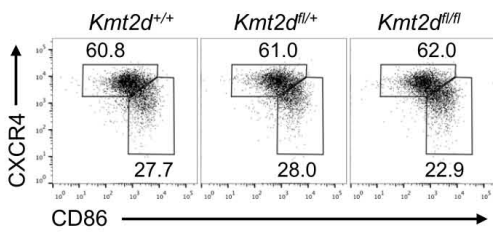
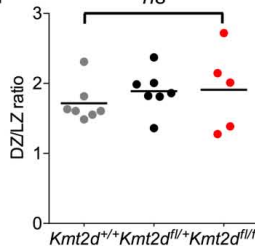
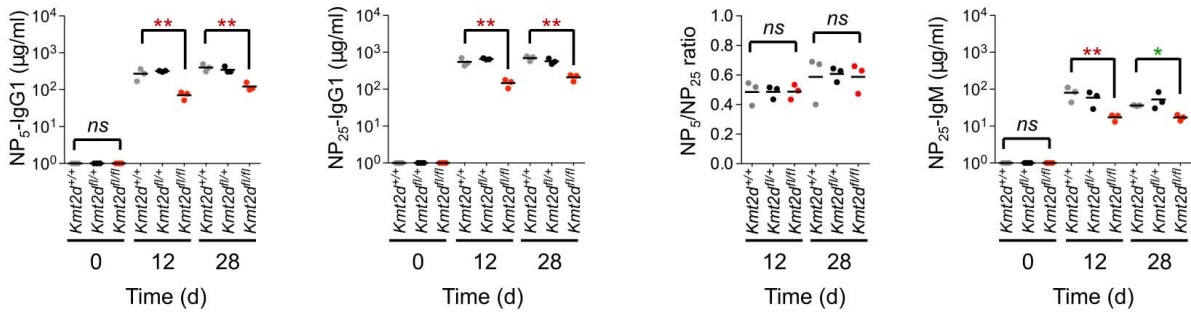
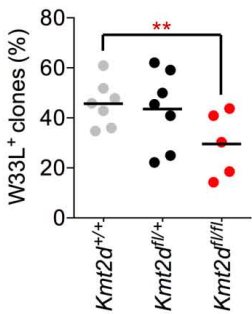
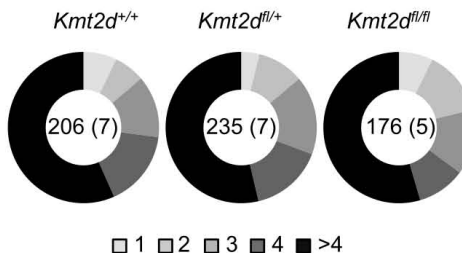
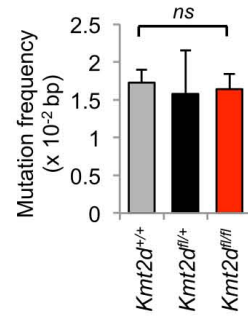


b



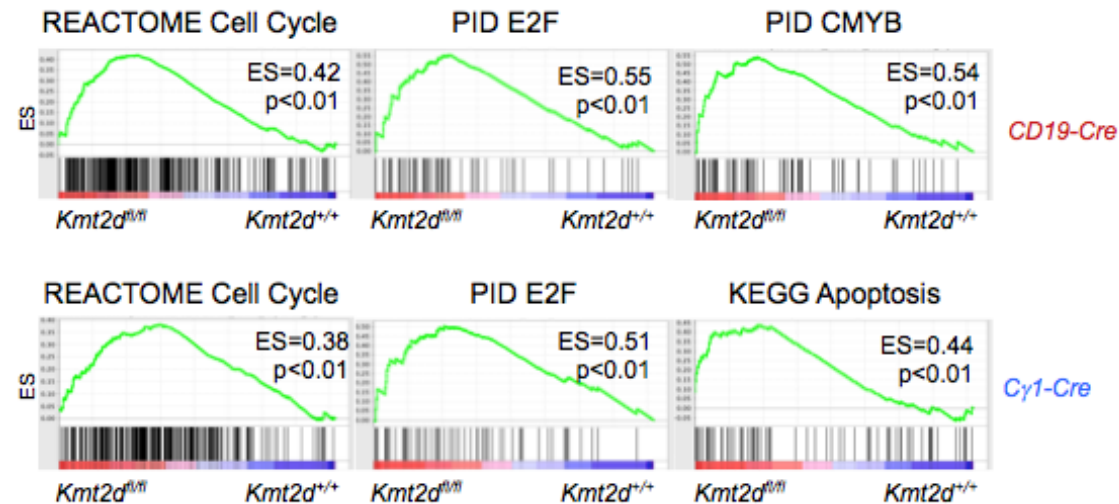
c



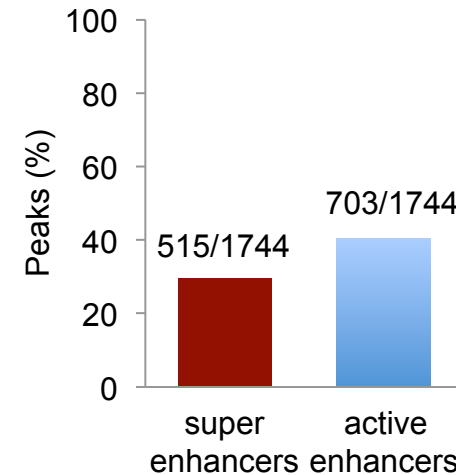
a**b****c****d****e****f****g****h**

Supplementary Fig. 10

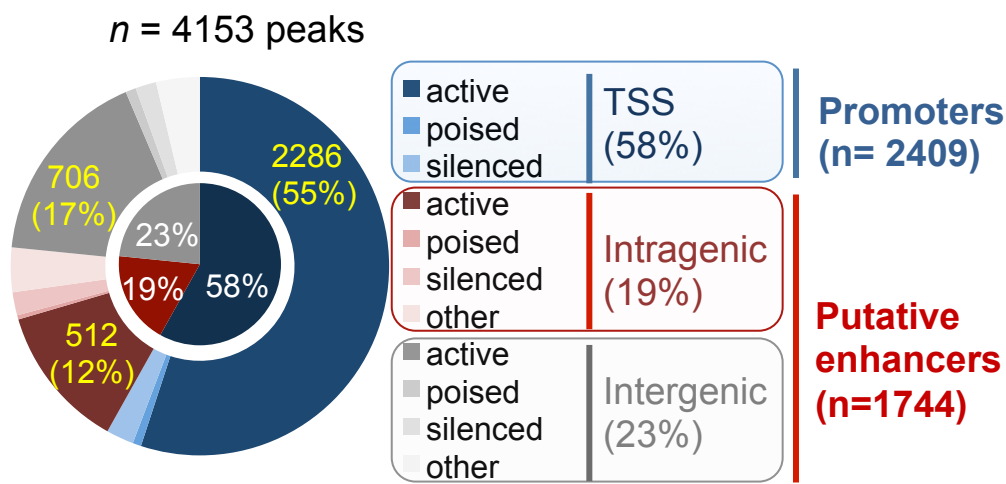
a



c

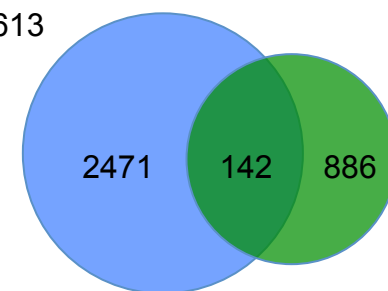


b



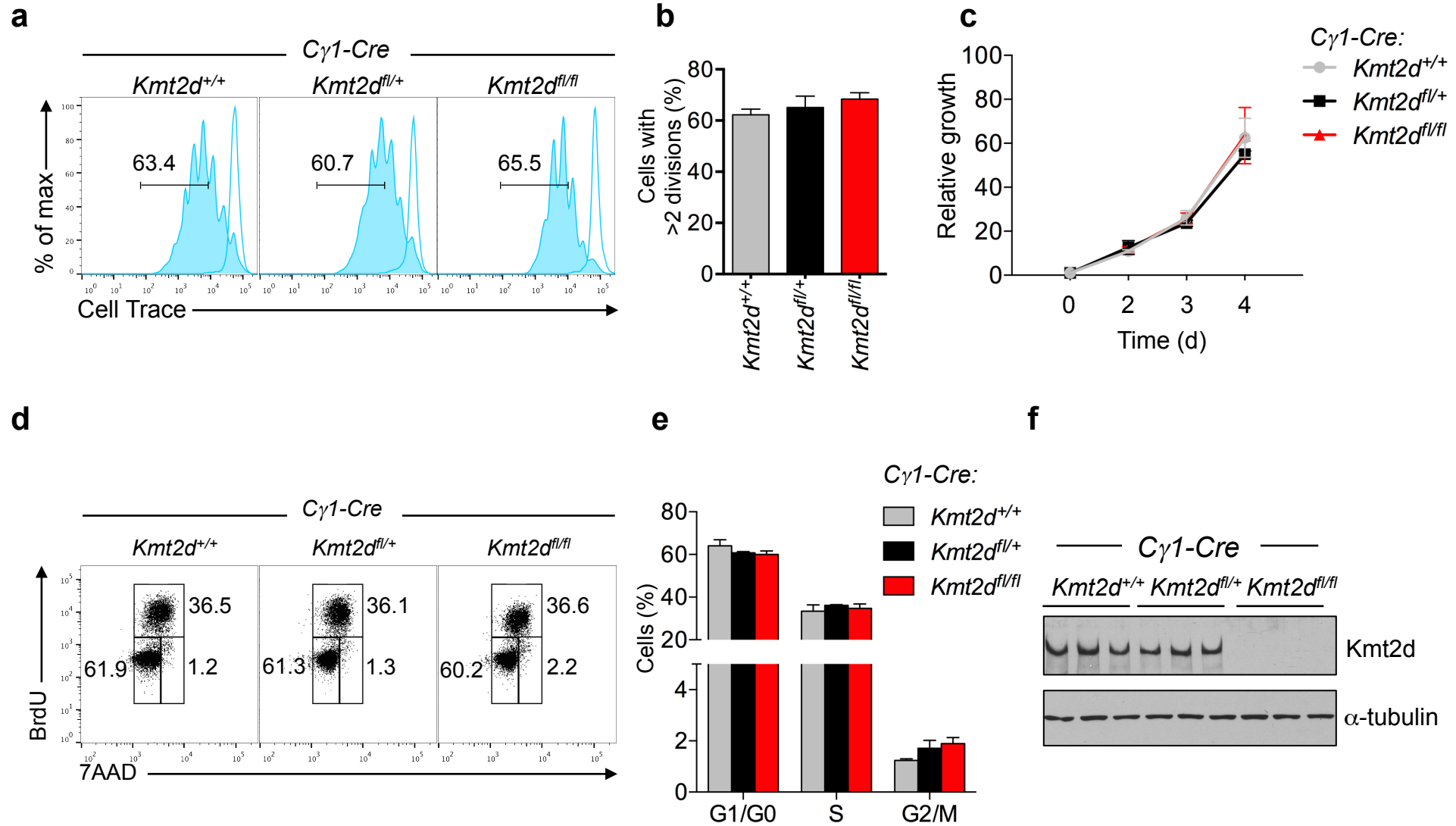
d

KMT2D-bound
Active chromatin state
Conserved in mouse
 $n = 2613$



Down-regulated in
 $Kmt2d^{fl/fl}$ vs $Kmt2d^{+/+}$ CD19-Cre
 $n = 1028$

Supplementary Fig. 11



Supplementary Table 1. Genes differentially expressed in *Kmt2d*^{f/f} vs *Kmt2d*^{t/t} GC B cells (FDR ≤ 0.15, FC ≥ 1.5)

Gene symbol	ProbeID	p value*	fdr	fold change
Downregulated in <i>Kmt2d</i>^{f/f} CD19-Cre				
Ticam1	1454676_s_at	0.000003	0.039846	0.662934
Apoe	1432466_a_at	0.000008	0.041126	0.297587
Pacsin1	1449381_a_at	0.000010	0.042049	0.269060
Pld4	1433678_at	0.000012	0.043962	0.333870
Ncf4	1418465_at	0.000037	0.087346	0.529985
Ankrd11	1460020_at	0.000059	0.093092	0.463267
Ncf1	1456772_at	0.000062	0.093092	0.324228
Apoc2	1418069_at	0.000074	0.094525	0.235462
Cotl1	1425801_x_at	0.000082	0.094525	0.544516
Igf2bp2	1437103_at	0.000088	0.094525	0.408192
Cwc27	1426455_at	0.000088	0.094525	0.513572
Gna12	1455008_at	0.000117	0.109074	0.490130
Sh3pxd2a	1428914_at	0.000124	0.111487	0.454421
9930012K11Rik	1433801_at	0.000130	0.111516	0.303367
Dkk1	1417787_at	0.000141	0.112631	0.635158
Neurl3	1444003_at	0.000158	0.115183	0.345169
D830036C21Rik	1446634_at	0.000200	0.115183	0.453945
Fes	1427368_x_at	0.000200	0.115183	0.494017
Dyrk3	1424229_at	0.000203	0.115183	0.410364
Evl	1434920_a_at	0.000213	0.115183	0.637859
Mgat4a	1435641_at	0.000222	0.115183	0.595227
Bmyc	1428669_at	0.000227	0.115183	0.502979
Col15a1	1448755_at	0.000241	0.115183	0.141724
Cryz	1438610_a_at	0.000256	0.115183	0.302800
Ssbp3	1427917_s_at	0.000302	0.115183	0.668238
Gfi1b	1420399_at	0.000325	0.115183	0.445928
Cysltr1	1418944_at	0.000328	0.115183	0.410635
Ceacam1	1460682_s_at	0.000331	0.115183	0.581504
Lrrc56	1427890_a_at	0.000352	0.115183	0.359417
Kcnn4	1421038_a_at	0.000368	0.115183	0.555783
Syne1	1455225_at	0.000397	0.115183	0.472014
Usp2	1417168_a_at	0.000412	0.115183	0.361920
Tnni2	1416889_at	0.000437	0.118076	0.262060
Bmf	1454880_s_at	0.000439	0.118076	0.465114
Cap1	1417461_at	0.000473	0.121745	0.279823
Krt222	1434535_at	0.000473	0.121745	0.644714
Ermap	1418909_at	0.000488	0.121745	0.400531
Serpinf1	1416168_at	0.000489	0.121745	0.337148
Sh2d1b1	1423024_at	0.000523	0.121745	0.357734
Gm14446	1435529_at	0.000549	0.121745	0.244960
Sfxn5	1436618_at	0.000572	0.122857	0.586541
Baiap2l1	1451539_at	0.000602	0.122857	0.436066
Srpk3	1418798_s_at	0.000685	0.122857	0.372382
Parp1	1422502_at	0.000702	0.122857	0.632048
Itgb7	1418741_at	0.000711	0.122857	0.554041
4833439L19Rik	1422017_s_at	0.000715	0.122857	0.599674
Tmed6	1416490_at	0.000716	0.122857	0.287428
Arhgap4	1419296_at	0.000725	0.122857	0.662132
Heatr7b1	1456631_at	0.000755	0.122857	0.584063
BC021614	1424953_at	0.000780	0.122857	0.578005
Tarsl2	1434738_at	0.000798	0.122857	0.578399

Flt3	1419538_at	0.000855	0.122857	0.409310
Dennd2d	1438712_at	0.000870	0.122857	0.612217
Arhgef10	1452302_at	0.000874	0.122857	0.455610
Tspan32	1418398_a_at	0.000884	0.122857	0.524838
Cdkl2	1449229_a_at	0.000889	0.122857	0.642639
Gsn	1415812_at	0.000897	0.122857	0.327756
Spata13	1454656_at	0.000897	0.122857	0.436798
Rassf5	1422638_s_at	0.000910	0.122857	0.605733
Dedd2	1452070_at	0.000914	0.122857	0.581607
Rnase6	1430534_at	0.000929	0.122857	0.640526
Cyp4f18	1419219_at	0.000930	0.122857	0.505525
Dennd1c	1437121_at	0.000950	0.122857	0.582733
Aldh2	1448143_at	0.000998	0.122857	0.509399
Lta	1420353_at	0.001008	0.122857	0.429697
Cyth4	1460437_at	0.001011	0.122857	0.382201
Ralgds	1460634_at	0.001036	0.122857	0.485598
Kctd1	1422293_a_at	0.001044	0.122857	0.468444
Stxbp1	1420505_a_at	0.001051	0.122857	0.237063
Arhgap26	1444128_at	0.001073	0.122857	0.617216
Susd3	1428975_at	0.001095	0.122857	0.609552
Scn8a	1423515_at	0.001156	0.122857	0.304512
Tox	1442039_at	0.001171	0.122857	0.635345
Rab30	1426452_a_at	0.001179	0.122857	0.656881
Lrrk2	1431394_a_at	0.001204	0.122857	0.603417
Arhgap39	1447521_x_at	0.001215	0.122857	0.503303
Aldh3b1	1452301_at	0.001266	0.123387	0.614439
4930403N07Rik	1456101_at	0.001285	0.124001	0.246991
Adap1	1433556_at	0.001321	0.125247	0.461535
Tnf	1419607_at	0.001356	0.125247	0.568956
D6Mm5e	1449358_at	0.001399	0.127969	0.462748
Ccdc23	1425616_a_at	0.001465	0.129322	0.580510
Dpm3	1452729_at	0.001478	0.129322	0.564372
Slc37a4	1417042_at	0.001509	0.130987	0.666484
Alad	1424877_a_at	0.001526	0.131958	0.619281
Il28ra	1460598_at	0.001577	0.132943	0.420911
Bfsp2	1434463_at	0.001618	0.133532	0.519997
Ccbp2	1422112_at	0.001638	0.133545	0.385012
Tmem38b	1449677_s_at	0.001646	0.133583	0.660591
Lck	1457917_at	0.001682	0.133583	0.512150
Psen2	1425869_a_at	0.001682	0.133583	0.561669
Abca1	1421840_at	0.001712	0.133749	0.399503
Sh3bp2	1448328_at	0.001749	0.134435	0.542093
Lrrc3	1431251_at	0.001798	0.136498	0.402640
Fcer2a	1451713_a_at	0.001858	0.138368	0.369498
Tnfaip8l2	1452948_at	0.001868	0.138381	0.557022
Lcp2	1418641_at	0.001914	0.139016	0.276686
Klhl32	1458375_at	0.001936	0.139362	0.522706
Traf5	1448861_at	0.001983	0.140728	0.570262
Gimap6	1427891_at	0.002003	0.141389	0.630796
Lhfpl4	1436553_at	0.002013	0.141588	0.660306
Coro2b	1434755_at	0.002145	0.146091	0.561899
Lyl1	1419120_at	0.002184	0.147329	0.439597
B230312A22Rik	1434059_at	0.002196	0.147329	0.484829
Myom1	1420693_at	0.002226	0.147329	0.508393
Pear1	1445223_at	0.002279	0.147903	0.211755

Ehf	1451375_at	0.002282	0.147903	0.336702
Ppdpf	1428381_a_at	0.002288	0.147903	0.605023
Ifngr1**	1448167_at	0.008728	0.213664	0.654415
Ptpn6**	1460188_at	0.019081	0.270387	0.866370

Upregulated in *Kmt2d*^{fl/fl} CD19-Cre

Trps1	1438214_at	0.000005	0.039846	5.719345
Spred1	1423161_s_at	0.000016	0.047980	2.429333
B930068K11Rik	1441656_at	0.000045	0.093092	2.592743
Slc39a8	1416832_at	0.000059	0.093092	5.360401
Gfi1	1417679_at	0.000065	0.093092	6.510079
Mpzl1	1428168_at	0.000092	0.094525	1.866629
Raph1	1434302_at	0.000104	0.101539	2.225907
Cnrip1	1433695_at	0.000135	0.111516	4.015501
Thyn1	1438480_a_at	0.000201	0.115183	1.833235
Dnaja4	1418591_at	0.000215	0.115183	4.647323
Vangl2	1436118_at	0.000224	0.115183	1.554177
Tifa	1426501_a_at	0.000246	0.115183	3.512753
Tmem55a	1424293_s_at	0.000246	0.115183	4.191568
Tnfrsf21	1450731_s_at	0.000259	0.115183	3.967112
Crhbp	1436127_at	0.000271	0.115183	2.773489
Dse	1455795_at	0.000278	0.115183	5.782651
Prkar2b	1438664_at	0.000284	0.115183	7.261130
Cdk6	1435338_at	0.000298	0.115183	2.106462
5930405F01Rik	1441372_at	0.000300	0.115183	2.360532
Mcf2l	1434140_at	0.000310	0.115183	8.391065
Cln6	1454837_at	0.000324	0.115183	1.524679
Slc35f5	1452059_at	0.000328	0.115183	2.094409
Rab39b	1435014_at	0.000341	0.115183	2.169307
Tsc22d1	1435952_at	0.000345	0.115183	5.596873
Jazf1	1433894_at	0.000366	0.115183	2.067252
Slc25a24	1452717_at	0.000374	0.115183	11.627258
Bcl2l1	1426191_a_at	0.000378	0.115183	1.731647
Kank2	1460559_at	0.000380	0.115183	3.514993
Enc1	1420965_a_at	0.000398	0.115183	2.618898
5230400M03Rik	1437493_at	0.000412	0.115183	2.344464
Dcbld1	1449291_a_at	0.000417	0.115183	1.882281
Acp12	1456735_x_at	0.000490	0.121745	3.971525
Trio	1439552_at	0.000502	0.121745	1.744497
Ttll1	1426427_at	0.000523	0.121745	1.908434
Fgf13	1418497_at	0.000544	0.121745	7.072004
Whrn	1432555_at	0.000548	0.121745	1.973475
Sdc1	1415943_at	0.000554	0.121745	1.567728
Slc4a8	1419851_at	0.000588	0.122857	2.136622
Socs2	1418507_s_at	0.000594	0.122857	3.416298
Mt1	1422557_s_at	0.000610	0.122857	2.260762
Tfdp2	1443962_at	0.000629	0.122857	2.897201
Arsb	1429189_at	0.000633	0.122857	3.422205
Trip10	1418092_s_at	0.000662	0.122857	1.542371
6720422M22Rik	1437798_at	0.000668	0.122857	4.843248
Epb4.1l5	1439284_at	0.000689	0.122857	3.284635
Tmtc4	1428113_at	0.000704	0.122857	1.863567
Rap2a	1426965_at	0.000784	0.122857	3.575768
Dtx4	1436545_at	0.000798	0.122857	2.131247
Neurl1b	1435564_at	0.000812	0.122857	2.254230

Anxa10	1449426_a_at	0.000863	0.122857	3.783719
Utrn	1452222_at	0.000872	0.122857	2.891853
Pdgfc	1419123_a_at	0.000892	0.122857	2.005919
Cd38	1450136_at	0.000915	0.122857	1.794804
Zfp365	1433583_at	0.000929	0.122857	2.913980
Pbx3	1447640_s_at	0.000959	0.122857	2.370866
1600021P15Rik	1439014_at	0.000976	0.122857	3.730182
Nudt4	1449107_at	0.000985	0.122857	1.737732
Cmpk2	1450484_a_at	0.000998	0.122857	3.424907
L3mbtl3	1454882_at	0.001000	0.122857	1.546259
Cnksr3	1433983_at	0.001003	0.122857	2.571336
Tex14	1419240_at	0.001009	0.122857	3.373259
Mxi1	1450376_at	0.001011	0.122857	2.490879
Fndc3b	1452783_at	0.001016	0.122857	1.719089
Clip3	1430543_at	0.001049	0.122857	2.175538
Bicd1	1438701_at	0.001069	0.122857	3.225699
Scmh1	1426241_a_at	0.001080	0.122857	1.804944
Lifr	1454984_at	0.001138	0.122857	5.664788
Capn5	1418671_at	0.001139	0.122857	3.041540
5830426K05Rik	1432808_at	0.001146	0.122857	2.614841
Slc1a4	1423549_at	0.001179	0.122857	1.587813
2900054C01Rik	1429625_at	0.001188	0.122857	2.653287
Gpatch2	1440329_s_at	0.001192	0.122857	1.845937
Ccdc88a	1445440_at	0.001195	0.122857	2.035601
Irf4	1421173_at	0.001197	0.122857	1.559925
Serpina3g	1424923_at	0.001216	0.122857	2.441810
Chd3	1428466_at	0.001220	0.122857	1.746032
Tjp2	1434599_a_at	0.001233	0.122857	2.445430
B3gnt8	1425128_at	0.001267	0.123387	1.769762
Csrnp2	1434532_at	0.001298	0.124731	1.670252
Tmem2	1424711_at	0.001325	0.125247	1.942017
Acot11	1429267_at	0.001331	0.125247	3.072212
5830456J23Rik	1433168_x_at	0.001344	0.125247	1.887939
Lpcat2	1434945_at	0.001350	0.125247	2.400610
Zeb2	1434298_at	0.001355	0.125247	3.229939
Inpp4b	1457359_at	0.001368	0.125804	1.802482
Klf7	1419356_at	0.001478	0.129322	1.505723
4933404O12Rik	1435827_at	0.001581	0.132943	1.878199
Sbk1	1451190_a_at	0.001594	0.133439	1.696274
Pfkm	1416780_at	0.001606	0.133439	1.664423
Neto2	1436309_at	0.001619	0.133532	1.727825
Sord	1426584_a_at	0.001633	0.133545	1.745790
Atrnl1	1449666_at	0.001638	0.133545	1.814545
A630081D01Rik	1457759_at	0.001657	0.133583	1.851094
Klh122	1426481_at	0.001683	0.133583	4.557507
Cox4i2	1421373_at	0.001716	0.133749	2.081574
Pkp4	1452209_at	0.001721	0.133749	1.525943
Fam135a	1453122_at	0.001744	0.134435	3.059778
Kif5c	1455266_at	0.001836	0.137805	5.627675
Klh13	1448269_a_at	0.001850	0.138256	5.325914
Eno2	1418829_a_at	0.001878	0.138402	3.213290
Ptpn9	1451037_at	0.001896	0.139016	1.846406
Aim1	1426942_at	0.001907	0.139016	2.145582
Snhg3	1433789_at	0.001925	0.139016	1.656661
Slc9a3r2	1439369_x_at	0.001950	0.139902	2.117645

Gad1	1416561_at	0.002104	0.144618	2.533160
Stom	1438910_a_at	0.002110	0.144618	1.878258
Cmtm4	1434337_at	0.002205	0.147329	1.525354
Ctdspl	1422510_at	0.002213	0.147329	2.473329
E430022K19Rik	1440072_at	0.002221	0.147329	2.068041
Kdm1b	1433649_at	0.002227	0.147329	1.631807
Armcx4	1427167_at	0.002269	0.147903	2.796050
Egln3	1418649_at	0.002280	0.147903	16.269365
Cdr2	1417430_at	0.002366	0.149799	1.528175
Bcl2**	1437122_at	0.012848	0.240995	1.824748
Ccnf**	1422513_at	0.012961	0.241339	1.272240
Myb**	1422734_a_at	0.013172	0.242401	2.056670
Ccnd3**	1415907_at	0.049527	0.354823	1.088617

Downregulated in *Kmt2d^{fl/fl} Cy1-Cre*

A630023P12Rik	1455370_at	0.000221	0.126659	0.127203
Gm14446	1435529_at	0.000015	0.080300	0.198641
Tnni2	1416889_at	0.000053	0.095404	0.251682
Gsn	1437171_x_at	0.000140	0.116204	0.440043
Aif1	1418204_s_at	0.000155	0.119322	0.453986
Tspan1	1417957_a_at	0.000240	0.126659	0.458170
Pear1	1425268_a_at	0.000592	0.146714	0.467393
Lyl1	1419120_at	0.000296	0.141731	0.492052
Dnase1	1424592_a_at	0.000015	0.080300	0.499373
Atxn7l1	1428279_a_at	0.000202	0.126393	0.536659
Ralgds	1460634_at	0.000109	0.106378	0.538639
Evl	1450106_a_at	0.000490	0.146714	0.558241
Kcnn4	1421038_a_at	0.000372	0.146714	0.567439
Fmn1l3	1426825_at	0.000076	0.095404	0.616541
Acap1	1434873_a_at	0.000549	0.146714	0.629693
Arhgap9	1449619_s_at	0.000205	0.126393	0.638321
Syngr2	1448577_x_at	0.000025	0.080300	0.650321

Upregulated in *Kmt2d^{fl/fl} Cy1-Cre*

Serpini1	1448443_at	0.000418	0.146714	1.516002
Praf2	1416781_at	0.000075	0.095404	1.551799
Nucb1	1416903_at	0.000105	0.106378	1.553996
Trib2	1426640_s_at	0.000114	0.106378	1.568599
Zdhhc8	1451476_at	0.000119	0.106802	1.585230
Gpr171	1438439_at	0.000089	0.095481	1.665986
Zfyve21	1424670_s_at	0.000353	0.146714	1.673706
E130303B06Rik	1434981_at	0.000488	0.146714	1.703563
Flot2	1417544_a_at	0.000041	0.095404	1.714584
Vcl	1416156_at	0.000074	0.095404	1.738571
Hist1h2bc	1418072_at	0.000027	0.080300	1.764758
Thap11	1416428_at	0.000068	0.095404	1.768897
Txnrdr2	1429971_at	0.000030	0.080300	1.775683
4930523C07Rik	1437900_at	0.000240	0.126659	1.781490

Nqo2	1449983_a_at	0.000425	0.146714	1.844273
Prkca	1450945_at	0.000013	0.080300	1.845828
4930562F07Rik	1453557_at	0.000568	0.146714	1.856303
Dcbld1	1449291_a_at	0.000320	0.146067	1.896227
Tnfrsf21	1422740_at	0.000197	0.126393	1.932169
Gemin8	1424587_at	0.000182	0.126393	1.963838
P4htm	1459807_x_at	0.000190	0.126393	1.965283
Klhl14	1428837_at	0.000578	0.146714	1.976577
Tox2	1440156_s_at	0.000237	0.126659	2.020287
Tfdp2	1435344_at	0.000367	0.146714	2.021673
Scmh1	1426241_a_at	0.000484	0.146714	2.073052
Aim1	1426942_at	0.000027	0.080300	2.079614
Lmo4	1420981_a_at	0.000456	0.146714	2.214747
Gpt2	1438385_s_at	0.000575	0.146714	2.230214
Agpat4	1436640_x_at	0.000356	0.146714	2.236990
Prkce	1449956_at	0.000284	0.138776	2.440390
Il15ra	1448681_at	0.000513	0.146714	2.543214
Spred1	1460116_s_at	0.000327	0.146067	2.639219
Cnrip1	1433695_at	0.000542	0.146714	2.764054
Il12a	1425454_a_at	0.000234	0.126659	2.867877
Rcn1	1417090_at	0.000147	0.117434	2.884699
Mxi1	1450376_at	0.000060	0.095404	3.313973
Plin2	1448318_at	0.000265	0.132873	3.630301
Fmn2	1450063_at	0.000053	0.095404	4.425410
Bik	1420362_a_at	0.000128	0.110077	5.274766
Ppm1e	1434990_at	0.000248	0.127184	5.454016
Slc25a24	1452717_at	0.000505	0.146714	6.465133
Lphn2	1434111_at	0.000190	0.126393	7.116062
Prkar2b	1456475_s_at	0.000012	0.080300	7.499940

* Genes that are upregulated or downregulated in *Kmt2d*^{f/f} GC B cells are ordered by decreasing p value (most significant first).

** These genes were filtered out when using FDR < 0.15 and do not appear in Figure 4a, but were in the leading edge of the GSEA analysis or had a significant z score (Klein et al, J Exp Med 194(11):1625, 2001), and were experimentally validated.

Supplementary Table 2. Results of GSEA in *Kmt2d*-deficient vs *Kmt2d*-proficient GC B cells from *CD19-Cre* and *Cγ1-Cre* conditional knock-out mouse models (FDR ≤ 0.15)

NAME	SIZE	ES	NES	NOM p-val	FDR q-val	FWER p-val	RANK AT MAX	LEADING EDGE
CD19-Cre								
PID_CMYB_PATHWAY	71	0.543654	1.950194	0.0000	0.065520	0.226	4572	tags=51%, list=22%, signal=65%
KEGG_CELL_CYCLE	104	0.501598	1.955438	0.0000	0.082497	0.213	5415	tags=58%, list=27%, signal=78%
PID_ECADHERIN_STABILIZATION_PATHWAY	38	0.589301	1.893744	0.0000	0.104014	0.387	1734	tags=37%, list=8%, signal=40%
REACTOME_CELL_CYCLE_MITOTIC	238	0.429217	1.856588	0.0000	0.104243	0.556	5804	tags=49%, list=28%, signal=68%
PID_E2F_PATHWAY	60	0.557519	1.963463	0.0000	0.108485	0.189	5474	tags=67%, list=27%, signal=91%
REACTOME GLUTATHIONE_CONJUGATION	17	0.701870	1.862956	0.0000	0.111402	0.532	1165	tags=29%, list=6%, signal=31%
REACTOME_CELL_CYCLE	278	0.422109	1.866512	0.0000	0.123485	0.512	5804	tags=50%, list=28%, signal=68%
BIOCARTA_CELLCYCLE_PATHWAY	18	0.730172	1.989455	0.0000	0.149263	0.134	3555	tags=67%, list=17%, signal=81%
BIOCARTA_TID_PATHWAY	19	-0.686489	-1.975277	0.0000	0.125120	0.122	3494	tags=53%, list=17%, signal=63%
Cγ1-Cre								
BIOCARTA_CELLCYCLE_PATHWAY	18	0.743367	2.244506	0.0000	0.003773	0.003	4774	tags=78%, list=23%, signal=101%
BIOCARTA_G1_PATHWAY	25	0.585642	1.930435	0.0018	0.069507	0.366	2966	tags=48%, list=15%, signal=56%
PID_HIF2PATHWAY	27	0.593471	1.969234	0.0000	0.070028	0.244	2361	tags=37%, list=12%, signal=42%
REACTOME_CELL_CYCLE	278	0.382640	1.920625	0.0000	0.072038	0.412	7518	tags=54%, list=37%, signal=84%
REACTOME_DOWNSTREAM_SIGNAL_TRANSDUCTION	75	0.467728	1.948533	0.0000	0.072357	0.294	3597	tags=39%, list=18%, signal=47%
REACTOME_CELL_CYCLE_MITOTIC	236	0.404774	2.006803	0.0000	0.072787	0.164	7350	tags=53%, list=36%, signal=82%
REACTOME_PI3K_AKT_ACTIVATION	27	0.580417	1.932224	0.0018	0.077426	0.359	4600	tags=63%, list=23%, signal=81%
REACTOME_G1_PHASE	25	0.602355	1.971077	0.0018	0.084677	0.239	5726	tags=64%, list=28%, signal=89%
REACTOME_SIGNALING_BY_ERBB4	66	0.473495	1.884934	0.0034	0.097364	0.555	4900	tags=52%, list=24%, signal=68%
PID_E2F_PATHWAY	60	0.506870	2.012756	0.0000	0.099070	0.150	5157	tags=50%, list=25%, signal=67%
REACTOME_TRIGLYCERIDE BIOSYNTHESIS	29	0.549883	1.859584	0.0000	0.113584	0.648	2127	tags=34%, list=10%, signal=38%
REACTOME_BRANCHED_CHAIN_AMINO_ACID_CATABOLISM	15	0.645522	1.848912	0.0019	0.115900	0.689	5644	tags=80%, list=28%, signal=110%
REACTOME_TELOMERE_MAINTENANCE	32	0.527530	1.815968	0.0017	0.120468	0.790	4970	tags=44%, list=24%, signal=58%
KEGG_CELL_CYCLE	104	0.417187	1.819300	0.0000	0.124103	0.781	7178	tags=59%, list=35%, signal=90%
REACTOME_GLUTATHIONE_CONJUGATION	17	0.618669	1.833093	0.0088	0.125066	0.730	2030	tags=41%, list=10%, signal=46%
KEGG_SNARE_INTERACTIONS_IN_VESICULAR_TRANSPORT	31	0.519897	1.761862	0.0069	0.131274	0.911	6558	tags=65%, list=32%, signal=95%
KEGG_APOPTOSIS	71	0.438341	1.820706	0.0000	0.131514	0.777	4608	tags=46%, list=23%, signal=60%
PID_HIF1_TFPATHWAY	54	0.446694	1.762191	0.0017	0.136435	0.909	3584	tags=37%, list=18%, signal=45%
REACTOME_REGULATION_OF_HYPOXIA_INDUCIBLE_FACTOR_HIF_BY_OXYGEN	17	0.617101	1.767193	0.0125	0.136823	0.899	603	tags=24%, list=3%, signal=24%
PID_FOXM1PATHWAY	36	0.494476	1.752324	0.0088	0.137616	0.927	3211	tags=36%, list=16%, signal=43%
KEGG_P53_SIGNALING_PATHWAY	56	0.456657	1.796470	0.0034	0.138026	0.840	4608	tags=43%, list=23%, signal=55%
REACTOME_MITOTIC_G2_G2_M_PHASES	61	0.447349	1.769318	0.0017	0.140982	0.893	4636	tags=39%, list=23%, signal=51%
REACTOME_PI1_METABOLISM	33	0.515581	1.778985	0.0018	0.143025	0.876	6355	tags=70%, list=31%, signal=101%
REACTOME_GPCR_LIGAND_BINDING	308	-0.380297	-2.072433	0.0000	0.010659	0.065	5134	tags=45%, list=25%, signal=59%
KEGG_NEUROACTIVE_LIGAND_RECECTOR_INTERACTION	216	-0.409664	-2.164495	0.0000	0.010923	0.017	5967	tags=51%, list=29%, signal=71%
REACTOME_CLASS_A1_RHODOPSIN_LIKE_RECEPTEORS	216	-0.400409	-2.100944	0.0000	0.013931	0.042	5134	tags=45%, list=25%, signal=59%
REACTOME_POTASSIUM_CHANNELS	81	-0.446515	-2.022097	0.0000	0.016841	0.123	5397	tags=52%, list=26%, signal=70%
REACTOME_PEPTIDE_LIGAND_BINDING_RECEPTEORS	139	-0.415555	-2.004090	0.0000	0.017725	0.155	5134	tags=47%, list=25%, signal=62%
REACTOME_VOLTAGE_GATED_POTASSIUM_CHANNELS	34	-0.520124	-1.929467	0.0021	0.036506	0.327	5339	tags=59%, list=26%, signal=79%
KEGG_TRYPTOPHAN_METABOLISM	35	-0.505457	-1.871164	0.0000	0.052924	0.530	2655	tags=34%, list=13%, signal=39%
REACTOME_GENERATION_OF_SECOND_MESSENGER_MOLECULES	19	-0.574742	-1.813437	0.0089	0.075349	0.722	1170	tags=32%, list=6%, signal=33%
KEGG_CYTOKINE_CYTOKINE_RECECTOR_INTERACTION	196	-0.345847	-1.793787	0.0000	0.084008	0.782	3912	tags=39%, list=19%, signal=48%
KEGG_BASAL_CELL_CARCINOMA	52	-0.438365	-1.785135	0.0000	0.084579	0.810	4570	tags=54%, list=22%, signal=69%
REACTOME_FGFR_LIGAND_BINDING_AND_ACTIVATION	20	-0.548459	-1.772798	0.0022	0.086659	0.836	6753	tags=70%, list=33%, signal=104%
REACTOME_AMINE_LIGAND_BINDING_RECEPTEORS	27	-0.497085	-1.732143	0.0064	0.103832	0.925	5891	tags=59%, list=29%, signal=83%
REACTOME_EXTRACELLULAR_MATRIX_ORGANIZATION	75	-0.404416	-1.738111	0.0024	0.104459	0.919	5187	tags=47%, list=25%, signal=62%
REACTOME_CYTOCHROME_P450_ARRANGED_BY_SUBSTRATE_TYPE	26	-0.490908	-1.709116	0.0107	0.118923	0.968	2159	tags=42%, list=11%, signal=47%
BIOCARTA_COMP_PATHWAY	15	-0.560583	-1.689731	0.0179	0.124108	0.981	3861	tags=47%, list=19%, signal=57%
ST_MYOCYTE_AD_PATHWAY	24	-0.495677	-1.660017	0.0184	0.142900	0.995	3144	tags=46%, list=15%, signal=54%

Supplementary Table 3. List of KMT2D "core target" genes (bound by KMT2D in human GC B cells and downregulated in *CD19-Cre Kmt2d^{fl/fl}* GC B cells)

Note: this supplementary item has two worksheets: "KMT2D core target genes" and "DAVID pathway enrichment analysis"

Genomic Location (hg19)*	Best P-value (ChIPseeqer)	Gene Symbol	Distance from TSS (in bp)	Location relative to gene	Overlap to H3K4me3	Overlap to H3K27me3	Overlap to H3K4me1	Overlap to H3K27Ac	Overlap to predicted GC enhancer	Overlap to predicted GC superenhancer	Class	Expressed in Conserved Mouse human GC B cells	ProbeID	pvalue^	
chr17:66221548-66221649	-7.8	AMZ2	-22547	intergenic	-	-	+	+	Yes	Yes	active enhancer	+	Amz2	1417241_at	0.001466
chrX:37614409-37614550	-8.1	CYBB	-24791	intergenic	-	-	+	+	Yes	no	active enhancer	+	Cybb	1436778_at	0.019816
chr13:30906872-30907179	-14.4	KATNAL1	-25401	intergenic	-	-	+	+	Yes	Yes	active enhancer	+	Katnal1	1442348_at	0.043768
chr18:24018928-24019213	-22.7	KCTD1	109430	intergenic	-	-	+	+	Yes	no	active enhancer	+	Kctd1	1422293_a_at	0.001044
chr10:52122338-52122758	-14.8	SGMS1	-114178	intergenic	-	-	+	+	Yes	no	active enhancer	+	Sgms1	1442079_at	0.015466
chr20:46044182-46044284	-14.4	ZMYND8	-58600	intergenic	-	-	+	+	Yes	Yes	active enhancer	+	Zmynd8	1429415_at	0.030599
chr9:107686220-107686384	-6.6	ABCA1	4225	intragenic	-	-	+	+	Yes	no	active enhancer	+	Abca1	1421840_at	0.001712
chr11:44631013-44631014	-8.1	CD82	43872	intragenic	-	-	+	+	Yes	Yes	active enhancer	+	Cd82	1416401_at	0.006256
chr2:109228715-109228849	-13.3	LIMS1	5165	intragenic	-	-	+	+	Yes	Yes	active enhancer	+	Lims1	1418230_a_at	0.013210
chr19:2090153-2090767	-16.4	MOB3A	5809	intragenic	-	-	+	+	Yes	Yes	active enhancer	+	Mob3a	1434388_at	0.019631
chr7:102082126-102082378	-23.0	Orai2	8275	intragenic	-	-	+	+	Yes	Yes	active enhancer	+	Orai2	1434763_at	0.005741
chr11:82774363-82774608	-19.4	RAB30	8480	intragenic	-	-	+	+	Yes	Yes	active enhancer	+	Rab30	1426452_a_at	0.001179
chr17:55082338-55082808	-19.8	SCPEP1	27105	intragenic	-	-	+	+	Yes	no	active enhancer	+	Scpep1	1455908_a_at	0.006653
chr5:138945145-138945287	-17.1	UBE2D2	4465	intragenic	-	-	+	+	Yes	no	active enhancer	+	Ube2d2a	1416475_at	0.012286
chr1:220263127-220263313	-14.2	BPNT1	-25	promoter	+	-	-	+	no	no	active promoter	+	Bpnt1	1418764_a_at	0.009097
chr22:42947854-42947966	-7.6	SERHL2	-1958	promoter	+	-	+	+	Yes	Yes	active promoter	+	Serhl	1421938_at	0.007904
chrX:103401295-103401848	-75.5	SLC25A53	137	promoter	+	-	-	+	no	no	active promoter	+	Slc25a53	1459914_at	0.035298
chr22:23377043-23377412	-11.9	GNAZ	-35442	intergenic	-	-	+	+	Yes	no	active enhancer	+	Gnaz	1435268_at	0.021460
chr17:65809358-65809615	-14.4	BPTF	-12294	intergenic	-	-	+	+	Yes	Yes	active enhancer	+	Bptf	1439102_at	0.009451
chr2:68638485-68638741	-13.3	PLEK	46291	intragenic	-	-	+	+	Yes	no	active enhancer	+	Plek	1448749_at	0.008071
chr1:24517528-24517733	-11.8	IFNLR1	-3865	intragenic	-	-	+	+	Yes	Yes	active enhancer	+	Ifnlr1	1460598_at	0.001577
chr16:48278047-48278312	-31.8	LONP2	101	promoter	+	-	-	+	no	no	active promoter	+	Lonp2	1460178_at	0.017056
chr7:74188126-74188304	-7.9	NCF1	-94	promoter	+	-	+	+	no	no	active promoter	+	Ncf1	1456772_at	0.000062
chr7:40011620-40011739	-8.8	CDK13	21720	intragenic	-	-	+	+	Yes	no	active enhancer	+	Cdk13	1458313_at	0.023144
chr4:88343552-88343954	-49.6	NUDT9	4	promoter	+	-	-	+	no	no	active promoter	+	Nudt9	1441633_at	0.024497
chr7:66461666-66461953	-11.8	TYW1	17	promoter	+	-	-	-	no	no	active promoter	+	Tyw1	1426781_at	0.031998
chr19:19302751-19303191	-43.7	RFXANK	-37	promoter	+	-	-	+	no	no	active promoter	+	Rfxank	1425670_at	0.075395
chr1:157776754-157776856	-15.3	FCRL1	13135	intragenic	-	-	+	+	Yes	no	active enhancer	+	Fcrl1	1425062_at	0.005773
chr3:121714089-121714193	-13.3	ILDR1	26986	intragenic	-	-	+	+	Yes	no	active enhancer	+	Ildr1	1423276_at	0.003017
chr4:8442297-8442683	-50.1	ACOX3	-38	promoter	+	-	-	+	no	no	active promoter	+	Acox3	1437352_at	0.024034
chr19:7402747-7403107	-24.7	ARHGEF18	-57072	intergenic	-	-	+	+	Yes	Yes	active enhancer	+	Arhgef18	1440700_a_at	0.002363
chr2:216973788-216974246	-34.7	XRCC5	-3	promoter	+	-	-	+	no	no	active promoter	+	Xrcc5	1451968_at	0.034740
chr6:90529355-90529656	-25.7	MDN1	8	promoter	+	-	-	+	no	no	active promoter	+	Mdn1	1439585_at	0.019487
chr1:40858996-40859113	-12.4	SMAP2	37	promoter	-	-	+	+	Yes	Yes	active enhancer	+	Smap2	1450675_at	0.007430
chr9:136202894-136203141	-27.3	SURF6	30	promoter	+	-	-	+	no	no	active promoter	+	Surf6	1416864_at	0.023649
chr5:158690115-158690229	-10.4	UBLCP1	83	promoter	+	-	-	+	no	no	active promoter	+	Ublcp1	1429606_at	0.025317
chr18:3247601-3247775	-13.5	MYL12A	160	promoter	+	-	-	+	no	no	active promoter	+	Myl12b	1428609_at	0.058483
chr19:67773508-67773657	-10.6	VAV1	903	promoter	+	-	-	+	no	no	active promoter	+	Vav1	1422932_a_at	0.002917
chr19:6737247-6737381	-12.1	GPR108	319	promoter	+	-	-	+	no	no	active promoter	+	Gpr108	1426078_a_at	0.000964
chr1:28216906-28217066	-15.9	THEMIS2	17932	intergenic	-	-	+	+	Yes	no	active enhancer	+	Themis2	1427041_at	0.029857
chr8:142129700-142130042	-19.9	DENND3	-8849	intergenic	-	-	+	+	Yes	Yes	active enhancer	+	Dennd3	1435927_at	0.003758
chr22:32026404-32026782	-25.4	PISD	217	promoter	+	-	-	+	no	no	active promoter	+	Pisd	1460585_x_at	0.346571
chr7:50477989-50478054	-7.2	FIGNL1	40067	intergenic	-	-	+	+	Yes	no	active enhancer	+	Fignl1	1460746_at	0.041797
chr18:74814641-74814786	-7.0	MBP	30061	intragenic	-	-	+	+	Yes	no	active enhancer	+	Mbp	1425263_a_at	0.002413
chr17:19881075-19881388	-13.7	AKAP10	-62	promoter	+	-	-	+	no	no	active promoter	+	Akap10	1428482_at	0.003831
chr7:121012754-121013011	-12.2	FAM3C	23540	intragenic	-	-	+	+	Yes	Yes	active enhancer	+	Fam3c	1417953_at	0.007260
chr16:4674512-4674564	-6.7	MGRN1	-287	promoter	+	-	-	+	no	no	active promoter	+	Mgrn1	1431285_at	0.017074
chr17:617985-618202	-21.7	VPS53	3	promoter	+	-	-	-	no	no	active promoter	+	Vps53	1416989_at	0.028169
chr13:24789444-24789564	-9.9	SPATA13	39073	intergenic	-	-	+	+	Yes	no	active enhancer	+	Spata13	1454656_at	0.000897
chr16:81897401-81897553	-6.9	PLCG2	84614	intragenic	-	-	+	+	Yes	no	active enhancer	+	Plcg2	1426926_at	0.005755
chr13:28622014-28622171	-7.7	FLT3	52637	intragenic	-	-	+	+	Yes	no	active enhancer	+	Flt3	1419538_at	0.000855
chr3:53226864-53226997	-7.6	PRKCD	31707	intergenic	-	-	+	+	Yes	Yes	active enhancer	+	Prkcd	1442256_at	0.007299
chr20:4803267-4803465	-13.7	RASSF2	925	promoter	+	-	-	+	no	no	active promoter	+	Rassf2	1428392_at	0.002849
chr22:47170548-47170809	-12.9	TBC1D22A	12164	intragenic	-	-	+	+	Yes	Yes	active enhancer	+	Tbc1d22a	1423776_s_at	0.014747

chr1:27226685-27227086	-39.1	GPATCH3	77	promoter	+	-	-	+	no	no	active promoter	+	Gpatch3	1440406_at	0.038399
chr14:102785949-102786073	-22.7	ZNF839	-77	promoter	+	-	-	-	no	no	active promoter	+	Zfp839	1456886_at	0.007649
chr2:223520765-223521030	-15.2	FARSB	-70	promoter	+	-	-	+	no	no	active promoter	+	Farsb	1430986_at	0.017547
chr9:34126554-34126772	-16.4	DCAF12	108	promoter	+	-	-	+	Yes	no	active promoter	+	Dcaf12	1429392_at	0.003004
chr1:52870134-52870425	-16.8	PRPF38A	60	promoter	+	-	-	+	no	no	active promoter	+	Prpf38a	1444087_at	0.030321
chr16:70473184-70473349	-12.1	ST3GAL2	-275	promoter	+	-	-	-	no	no	active promoter	+	St3gal2	1421891_at	0.018174
chr2:99374649-99374834	-11.3	MGAT4A	-27152	intergenic	-	-	+	+	Yes	no	active enhancer	+	Mgat4a	1435641_at	0.000222
chr1:31227520-31227804	-23.8	LAPTM5	3021	intragenic	-	-	+	+	Yes	Yes	active enhancer	+	Laptm5	1417721_s_at	0.008349
chr8:81059178-81059200	-5.8	TPD52	24705	intragenic	-	-	+	+	Yes	Yes	active enhancer	+	Tpd52	1419494_a_at	0.001493
chr3:112709768-112709858	-6.2	GTPBP8	13	promoter	+	-	-	+	no	no	active promoter	+	Gtpbp8	1445419_at	0.044023
chr4:147096756-147096947	-13.0	LSM6	16	promoter	+	-	-	+	no	no	active promoter	+	Lsm6	1455926_at	0.042145
chr1:206785560-206785977	-78.2	EIF2D	136	promoter	+	-	-	-	no	no	active promoter	+	Eif2d	1436724_a_at	0.007826
chr14:7738584-7738844	-9.9	TMED8	4682	intragenic	-	-	+	+	Yes	Yes	active enhancer	+	Tmed8	1427622_at	0.011279
chr19:19266346-19266712	-17.8	MEF2B	14569	intragenic	-	-	+	+	Yes	Yes	active enhancer	+	Me2b	1421541_a_at	0.006088
chr16:69373436-69373702	-16.9	COG8	-43	promoter	+	-	-	+	no	no	active promoter	+	Cog8	1447860_x_at	0.010837
chr6:79577124-79577356	-22.1	IRAK1BP1	-21	promoter	+	-	-	+	no	no	active promoter	+	Irak1bp1	1431771_a_at	0.005331
chr12:40620092-40620261	-18.0	LRRK2	1363	intragenic	-	-	+	+	no	no	active enhancer	+	Lrrk2	1431394_a_at	0.001204
chr1:6614495-6614757	-35.1	NOL9	32	promoter	+	-	-	-	no	no	active promoter	+	Nol9	1432218_a_at	0.041695
chr5:64064368-64064958	-43.7	CWC27	-82	promoter	+	-	-	+	no	no	active promoter	+	Cwc27	1426455_at	0.000088
chr16:56976232-56976347	-7.5	HERPUD1	10287	intragenic	-	-	+	+	Yes	Yes	active enhancer	+	Herpud1	1435626_a_at	0.010185
chr1:151227048-151227322	-37.2	PSMD4	-12	promoter	+	-	-	-	no	no	active promoter	+	Psmd4	1425859_a_at	0.023847
chr16:10962604-10962798	-17.3	CIITA	-8354	intergenic	-	-	+	+	Yes	Yes	active enhancer	+	Ciita	1421210_at	0.033465
chr10:11720105-11720306	-8.8	ECHDC3	-64151	intergenic	-	-	+	+	Yes	Yes	active enhancer	+	Echdc3	1418862_at	0.019863
chr17:37009950-37010304	-57.7	RPL23	-74	promoter	+	-	-	+	no	no	active promoter	+	Rpl23	1422859_a_at	0.016185
chr2:55459451-55459873	-22.4	CLHC1	37	promoter	+	-	-	+	no	no	active promoter	+	1700034F02Rik	1438970_x_at	0.037161
chr1:14057292-14057645	-14.6	PRDM2	-18408	intergenic	-	-	+	+	Yes	Yes	active enhancer	+	Prdm2	1453068_at	0.025071
chr15:72978461-72978572	-6.5	BBS4	-4	promoter	+	-	-	-	no	no	active promoter	+	Bbs4	1434460_at	0.027143
chr1:111758752-111759062	-16.5	DENND2D	-11374	intergenic	-	-	+	+	Yes	no	active enhancer	+	Dennd2d	1438712_at	0.000870
chr11:71639459-71639920	-19.5	RNF121	-79	promoter	+	-	-	+	no	no	active promoter	+	Rnf121	1426503_a_at	0.008323
chr7:36231712-36232032	-13.5	EEDP1	39036	intragenic	-	-	+	+	Yes	Yes	active enhancer	+	Eepd1	1417877_at	0.021298
chr10:33403516-33403706	-14.2	ITGB1	-156318	intergenic	-	-	+	+	Yes	no	active enhancer	+	Itgb1	1427771_x_at	0.011200
chr2:74153977-74154108	-13.2	DGUOK	89	promoter	+	-	-	+	no	no	active promoter	+	Dguok	1425228_a_at	0.046576
chr11:33964845-33964963	-22.2	LMO2	-51068	intergenic	-	-	+	+	Yes	no	active enhancer	+	Lmo2	1454086_a_at	0.020647
chr5:17278153-17278538	-12.8	BASP1	60675	intergenic	-	-	+	+	Yes	Yes	active enhancer	+	Basp1	1428572_at	0.017367
chr4:79671298-79671667	-18.1	BMP2K	-26050	intergenic	-	-	+	+	Yes	no	active enhancer	+	Bmp2k	1458370_at	0.009972
chr1:6259552-6259903	-41.4	RPL22	-48	promoter	+	-	-	-	no	no	active promoter	+	Rpl22	1448398_s_at	0.024336
chr11:46722184-46722586	-36.4	ZNF408	68	promoter	+	-	-	-	no	no	active promoter	+	Zfp408	1457002_at	0.040996
chr7:77044926-77045030	-7.8	GSAP	739	promoter	+	-	-	+	no	no	active promoter	+	Gsap	1435596_at	0.032176
chr2:208890126-208890408	-14.5	PLEKHM3	17	promoter	+	-	-	-	no	no	active promoter	+	Plekhm3	1455331_at	0.002882
chr1:2322992-2323224	-23.9	MORN1	82	promoter	+	-	-	-	no	no	active promoter	+	Morn1	1456435_at	0.017434
chr3:47018103-47018394	-26.5	CCDC12	-257	promoter	+	-	-	+	no	no	active promoter	+	Ccdc12	1419803_s_at	0.004666
chr17:76143835-76143980	-12.1	C17orf99	1473	intragenic	-	-	+	+	no	no	active enhancer	+	6030468B19Rik	1431194_at	0.030260
chr22:18479459-18479625	-8.9	MICAL3	27783	intragenic	-	-	+	+	Yes	Yes	active enhancer	+	Mical3	1434221_at	0.163867
chr16:11862737-11863273	-59.1	TXNDC11	-26357	intergenic	-	-	+	+	Yes	Yes	active enhancer	+	Txndc11	1448782_at	0.025425
chr17:29641040-29641272	-10.6	EV12B	-26	promoter	+	-	-	+	Yes	Yes	active promoter	+	Evi2a-evi2b	1426505_at	0.017423
chr15:90437171-90437405	-18.6	AP3S2	329	promoter	+	-	-	-	no	no	active promoter	+	Ap3s2	1444413_at	0.045982
chr20:50077651-50077661	-7.4	NFATC2	81602	intergenic	-	-	+	+	Yes	no	active enhancer	+	Nfatc2	1439205_at	0.003309
chr17:56084513-56085091	-45.7	SRSF1	-95	promoter	+	-	-	+	no	no	active promoter	+	Srsf1	1457136_at	0.014137
chr1:161735952-161736262	-53.8	ATF6	73	promoter	+	-	-	+	no	no	active promoter	+	Atf6	1435444_at	0.011269
chr10:74008001-74008137	-13.6	DDIT4	-25608	intergenic	-	-	+	+	Yes	no	active enhancer	+	Ddit4	1428306_at	0.022583
chr1:40505494-40505706	-44.4	CAP1	-655	promoter	+	-	-	+	no	no	active promoter	+	Cap1	1417461_at	0.000473
chr10:26771223-26771376	-13.9	APBB1IP	44033	intragenic	-	-	+	+	Yes	no	active enhancer	+	Apbb1ip	1443145_at	0.010147
chr12:95867781-95868084	-14.7	METAP2	110	promoter	+	-	-	+	no	no	active promoter	+	Metap2	1436531_at	0.002067
chr9:115983488-115983702	-51.6	FKBP15	46	promoter	+	-	-	+	no	no	active promoter	+	Fkbp15	1439974_at	0.026453
chr1:226850624-226850882	-14.2	ITPKB	76123	intragenic	-	-	+	+	Yes	Yes	active enhancer	+	Itpkb	1435272_at	0.008428
chr20:30873680-30873869	-17.1	KIF3B	8320	intragenic	-	-	+	+	Yes	no	active enhancer	+	Kif3b	1450074_at	0.004387
chr17:47865815-47866034	-24.5	KAT7	-57	promoter	+	-	-	+	no	no	active promoter	+	Kat7	1459975_at	0.039414
chr7:1015087-1015235	-14.8	COX19	74	promoter	+	-	-	+	no	no	active promoter	+	Cox19	1434923_at	0.022947
chr7:101950383-101950491	-24.5	SH2B2	22084	intragenic	-	-	+	+	Yes	Yes	active enhancer	+	Sh2b2	1450718_at	0.009963
chr7:102036723-102036965	-18.5	PRKRIP1	40	promoter	+	-	-	-	no	no	active promoter	+	Prkrp1	1417425_at	0.026133

chr1:32859839-32860129	-24.5	BSDC1	78	promoter	+	-	-	-	no	no	active promoter	+	Bsdc1	1427270_a_at	0.008553
chr19:34760935-34761210	-14.9	KIAA0355	15616	intragenic	-	-	+	+	Yes	no	active enhancer	+	4931406P16Rik	1433993_at	0.022390
chr4:100730579-100730744	-12.6	DAPP1	-7320	intergenic	-	-	+	+	Yes	no	active enhancer	+	Dapp1	1421936_at	0.003980
chr16:30483854-30484008	-8.4	ITGAL	-52	promoter	+	-	-	+	Yes	Yes	active promoter	+	Itgal	1435560_at	0.022638
chr1:167586732-167587090	-20.8	RCSD1	-12563	intergenic	-	-	+	+	Yes	Yes	active enhancer	+	Rcsd1	1442866_at	0.025065
chr6:158185420-158185536	-14.9	SNX9	-58725	intergenic	-	-	+	+	Yes	Yes	active enhancer	+	Snx9	1423077_at	0.004288
chr1:211509264-211509374	-7.3	TRAF5	9171	intragenic	-	-	+	+	Yes	no	active enhancer	+	Traf5	1448861_at	0.001983
chr17:7387535-7387683	-8.4	ZBTB4	-41	promoter	+	-	-	+	no	no	active promoter	+	Zbtb4	1429722_at	0.011415
chr1:111682817-111682979	-16.4	DRAM2	-60	promoter	+	-	-	-	no	no	active promoter	+	Dram2	1453731_a_at	0.002534
chr18:77220531-77220646	-8.7	NFATC1	60314	intragenic	-	-	+	+	Yes	Yes	active enhancer	+	Nfatc1	1428479_at	0.004837
chr1:54873321-54873474	-10.7	SSBP3	-1329	promoter	+	-	-	-	no	no	active promoter	+	Ssbp3	1427917_s_at	0.000302
chr8:82059624-82059747	-8.0	PAG1	-35382	intergenic	-	-	+	+	Yes	no	active enhancer	+	Pag1	1456403_at	0.031647
chr7:106505703-106505871	-20.1	PIK3CG	-137	promoter	+	-	-	+	no	no	active promoter	+	Pik3cg	1422708_at	0.002859
chr6:137752198-137752346	-7.5	IFNGR1	167826	intergenic	-	-	+	+	Yes	Yes	active enhancer	+	Ifngr1	1448167_at	0.008728
chr10:94516288-94516547	-19.2	HHEX	66736	intergenic	-	-	+	+	Yes	Yes	active enhancer	+	Hhex	1423319_at	0.030484
chr1:42217054-42217211	-16.0	HIVEP3	167246	intragenic	-	-	+	+	Yes	no	active enhancer	+	Hivep3	1458802_at	0.003212
chr8:59956445-59956664	-16.7	TOX	75213	intragenic	-	-	+	+	Yes	Yes	active enhancer	+	Tox	1442039_at	0.001171
chr17:56296577-56296610	-7.1	MKS1	73	promoter	+	-	-	+	no	no	active promoter	+	Mks1	1435835_at	0.006489
chr3:187957048-187957266	-12.7	LPP	13964	intragenic	-	-	+	+	Yes	Yes	active enhancer	+	Lpp	1440167_s_at	0.057578
chr5:139049700-139049883	-14.8	CXXC5	21490	intragenic	-	-	+	+	Yes	Yes	active enhancer	+	Cxxc5	1448960_at	0.020029
chr14:75906818-75906937	-6.5	JDP2	8040	intragenic	-	-	+	+	Yes	no	active enhancer	+	Jdp2	1450350_a_at	0.005916
chr1:16693767-16693961	-16.7	SZRD1	339	promoter	+	-	-	+	no	no	active promoter	+	Szrd1	1434482_at	0.007671
chr19:46010628-46010732	-10.5	VASP	-8	promoter	+	-	-	+	Yes	no	active promoter	+	Vasp	1451097_at	0.013039
chr11:118691644-118691784	-12.0	DDX6	-29742	intergenic	-	-	+	+	Yes	no	active enhancer	+	Ddx6	1424598_at	0.026452
chr2:219135062-219135384	-32.2	PNKD	108	promoter	+	-	-	-	no	no	active promoter	+	Pnkd	1418746_at	0.006878
chr2:73298732-73298893	-8.1	SFXN5	153	promoter	+	-	-	-	no	no	active promoter	+	Sfxn5	1436618_at	0.000572
chr11:64512661-64512813	-10.7	RASGRP2	191	promoter	+	-	-	+	no	no	active promoter	+	Rasgrp2	1417804_at	0.011299
chr12:7063069-7063174	-12.54	PTPN6	2687	intragenic	-	-	+	+	Yes	no	active enhancer	+	Ptpn6	1460188_at	0.019081

* Genomic coordinates of the peaks commonly identified by ChIP-Seq analysis in two independent GC B cell pools.

^ Significance P value of differential expression in *Kmt2d*^{+/+} vs *Kmt2d*^{-/-} CD19-Cre GC B cells.

Supplementary Table 3. DAVID Pathway enrichment analysis of Kmt2d "core target genes"

Database	Term	N of genes in overlap	overlap (%)	P Value	Genes in overlap	List Total*	Fold Enrichment	Bonferroni	Benjamini	FDR q-value
PANTHER_PATHWAY	P00010:B cell activation	7	5.3	1.17E-05	PIK3CG, PTPN6, PLCG2, NFATC2, PRKCD, VAV1, NFATC1	20	11.751149	0.000432	0.000432	0.010482
KEGG_PATHWAY	mmu04670:Leukocyte transendothelial migration	9	6.9	5.99E-06	PIK3CG, ITGAL, CYBB, NCF1, PLCG2, MYL12B, ITGB1, VAV1, VASP	50	8.679328	0.000479	0.000479	0.006367
KEGG_PATHWAY	mmu04650:Natural killer cell mediated cytotoxicity	8	6.1	6.77E-05	PIK3CG, ITGAL, PTPN6, PLCG2, NFATC2, VAV1, IFNGR1, NFATC1	50	7.525246	0.005401	0.001803	0.071937
KEGG_PATHWAY	mmu04662:B cell receptor signaling pathway	7	5.3	5.27E-05	PIK3CG, PTPN6, DAPP1, PLCG2, NFATC2, VAV1, NFATC1	50	10.041500	0.004209	0.002107	0.056032
PANTHER_PATHWAY	P00031:Inflammation mediated by chemokine and cytokine signalling pathway	9	6.9	3.98E-04	PIK3CG, ITGAL, PLCG2, NFATC2, PRKCD, ITGB1, VAV1, IFNGR1, NFATC1	20	4.226527	0.014627	0.007340	0.356941
KEGG_PATHWAY	mmu04666:Fc gamma R-mediated phagocytosis	6	4.6	1.38E-03	PIK3CG, NCF1, PLCG2, PRKCD, VAV1, VASP	50	7.026122	0.104572	0.027236	1.457096

* Number of genes in the query list mapped to any gene set in the indicated category.

Note that only pathways with relevance to the B cell context are shown in Figure 4e, where terms were renamed for brevity.

Supplementary Table 4. Analysis of *IghV* gene rearrangements in B-NHLs of compound *Cγ1-Cre/VavP-Bcl2* mice

Mouse ID	Genotype	Histologic Diagnosis	status	V gene	JH gene	N of bp analyzed	N of mutations	% mutations
90LN	VavP-Bcl2/Kmt2d ^{f/f}	FL	C, M	J558	JH2	1223	36	2.94
533LN	VavP-Bcl2/Kmt2d ^{f/f}	DLBCL	C, M	J558	JH2	1223	32	2.62
315LN	VavP-Bcl2/Kmt2d ^{f/f}	early FL	C, M	J558	JH4	375	10	2.67
36LN	VavP-Bcl2/Kmt2d ^{f/+}	DLBCL	C, M	J558	JH3	823	6	0.73
6LN	VavP-Bcl2/Kmt2d ^{f/+}	FL	C, M	VH1-13	JH2	245	14	5.71
20LN	VavP-Bcl2/Kmt2d ^{f/+}	FL	C, M	VH7183	JH2	1222	12	0.98
487LN	VavP-Bcl2/Kmt2d ^{f/+}	early FL	C, M	J558	JH3	290	23	7.93
112LN	VavP-Bcl2/Kmt2d ^{+/+}	DLBCL	C, UM	J558	JH4	281	0	0

Abbreviations: LN, lymph node; C, clonal; M, mutated; UM, unmutated.

Supplementary Table 5. DLBCL cell lines used in the study

Cell line	Source
OCI-Ly1	Ontario Cancer Institute*
OCI-Ly3	Ontario Cancer Institute*
OCI-Ly4	Ontario Cancer Institute*
OCI-Ly7	Ontario Cancer Institute*
OCI-Ly8	Ontario Cancer Institute*
OCI-Ly10	Ontario Cancer Institute*
OCI-Ly18	Ontario Cancer Institute*
HBL1	Tohoku et al., J Exp Med 1988 ^{§*}
U2932	Amini et al., Leuk Lymphoma 2002 ^{§*}
RIVA (RI-1)	Th'ng et al., Int J Cancer 1987 [§]
RC-K8	DSMZ*
TOLEDO	ATCC
PFEIFFER	ATCC
SUDHL2	Stanford University ^{§*}
SUDHL4	Stanford University ^{^*}
SUDHL5	Stanford University [^]
SUDHL6	Stanford University ^{^*}
SUDHL7	Stanford University [^]
SUDHL10	Stanford University [^]
FARAGE	ATCC
HT-DHL8	Dr. M. Shipp (DFCI)*
WSU-NHL	DSMZ
BJAB	Dr. T. Gilmore (BU)*
DB	DSMZ*
Karpas 422	DSMZ
VAL	DSMZ

[^]Epstein et al., Cancer 1978; Hecht et al., Cancer Genet Cytogenet 1985. Kindly provided by Dr. M. Shipp (Dana Farber Cancer Institute).

[†]HT-DHL8 is a subclone of the published HT DLBCL cell line, which carries one additional *KMT2D* truncating mutation on the same allele harboring the reported missense mutation (Pasqualucci et al., Nat Gen 2011).

[§]Kind gift of Dr. L. Staudt (NCI).

*verified for identity.

Supplementary Table 6. Oligonucleotides used for qRT-PCR analysis

Oligonucleotide Name	Oligonucleotide Sequence	Organism
hKMT2D-Forward	5'-GTGCAGCAGAAGATGGTGAA-3'	<i>Homo sapiens</i>
hKMT2D-Reverse	5'-GCACAATGCTGTCAGGAGAA-3'	<i>Homo sapiens</i>
hACTB-Forward	5'-CATGTACGTTGCTATCCAGGC-3'	<i>Homo sapiens</i>
hACTB-Reverse	5'-CTCCTTAATGTCACGCACGAT-3'	<i>Homo sapiens</i>
mKmt2d-Forward	5'-GCTATCACCCGTACTGTGTCAACA-3'	<i>Mus musculus</i>
mKmt2d-Reverse	5'-CACACACGATACTCCACACAA-3'	<i>Mus musculus</i>
mActb-Forward	5'-ATGGAGGGGAATACAGCCC-3'	<i>Mus musculus</i>
mActb-Reverse	5'-TTCTTGCAGCTCCTCGTT-3'	<i>Mus musculus</i>
mTnf-Forward	5'-GAATGGGCTTCAATCTGGA-3'	<i>Mus musculus</i>
mTnf-Reverse	5'-GCACCTCAGGGAAAGAGTCTG-3'	<i>Mus musculus</i>
mTnf-Forward-1	5'-GGCCTTCCTACCTTCAGACC-3'	<i>Mus musculus</i>
mTnf-Reverse-1	5'-AGCAAAAGAGGAGGCAACAA-3'	<i>Mus musculus</i>
mBcl2-Forward	5'-CATCTGCAGAACCTCCCTGT-3'	<i>Mus musculus</i>
mBcl2-Reverse	5'-GCACTACCTGCGTTCTCCTC-3'	<i>Mus musculus</i>
mBcl2l1-Forward	5'-CCCCAGAAGAAACTGAAGCA-3'	<i>Mus musculus</i>
mBcl2l1-Reverse	5'-CCTGGGGTTATGTGAAGCTG-3'	<i>Mus musculus</i>
mCdk6-Forward	5'-GGCGTACCCACAGAAACCATA-3'	<i>Mus musculus</i>
mCdk6-Reverse	5'-AGGTAAAGGCCATCTGAAAAT-3'	<i>Mus musculus</i>
mCcnd3-Forward	5'-TCCGTACTCCAGCTGCTCTT-3'	<i>Mus musculus</i>
mCcnd3-Reverse	5'-AGCTAACGAGCGAAGCAAAG-3'	<i>Mus musculus</i>
mCcnf-Forward	5'-AAACCCATCCCTGTCTACCC-3'	<i>Mus musculus</i>
mCcnf-Reverse	5'-CCAGCAAGGGTTGAAGCTGT-3'	<i>Mus musculus</i>
mDedd2-Forward	5'-ACTCTGGGCTGATGCTGTCT-3'	<i>Mus musculus</i>
mDedd2-Reverse	5'-GCCCAGGTTGGTTAGATGAA-3'	<i>Mus musculus</i>
mlfngr1-Forward	5'-GCCTGCTGGTGGTAAAGAAA-3'	<i>Mus musculus</i>
mlfngr1-Reverse	5'-AGGAGCCAGAACGCGACAATA-3'	<i>Mus musculus</i>
mLta-Forward	5'-CTCCATCCTGACCGTTGTTT-3'	<i>Mus musculus</i>
mLta-Reverse	5'-GTCCGACCTAGACCCACAAA-3'	<i>Mus musculus</i>
mMyb-Forward	5'-GCCTGAATGTTCATCCGTTT-3'	<i>Mus musculus</i>
mMyb-Reverse	5'-AAGGCAGAAACTGGCTGTTG-3'	<i>Mus musculus</i>

Supplementary Table 7. List of anti-KMT2D antibodies used in the study

Note: this supplementary item has two worksheets: "anti-KMT2D antibodies" and "Antibodies used in FACS analysis".

Antibody name	Source	ID/Catalog #	Host	Reactivity	epitope (according to NP_003473.3)	Applications
KMT2D-a	Bethyl	BL1183	Rabbit	human	AA 650-700	IP
KMT2D-b	Bethyl	BL1184	Rabbit	human	AA 1625-1675	IP
KMT2D-c*	Bethyl	BL1185	Rabbit	human	AA 2725-2775	IP, WB
KMT2D-d	Bethyl	BL1186	Rabbit	human	AA 4025-4075	IP
KMT2D-e	Bethyl	BL1187	Rabbit	human	AA 1-50	IP
KMT2D-f	Bethyl	BL14312	Rabbit	human	available upon request	IP
KMT2D-g	Bethyl	BL14313	Rabbit	human	available upon request	IP
KMT2D-h	Bethyl	BL14317	Rabbit	human	available upon request	IP
KMT2D-S	Sigma-Aldrich	HPA035977	Rabbit	human	AA 4363-4494	IP, IHC, ChIP
ALR#4	Dr. Kai Ge, NIDDK	na	Rabbit	human	AA 4396-4559	WB
Kmt2d**	Diagenode	C15310100	Rabbit	mouse	central part of the protein	WB

* For brevity, this antibody is called KMT2D in Fig. 1 and Fig. 2.

** Commercial name: MII4.

Supplementary Table 7. List of antibodies used in FACS analysis

Antibody name	Source	Catalog #	clone #	Fluorochrome
BCL6	BD Pharmingen	561525	K112-91	Alex Fluo 647
CD4	BD Pharmingen	553051	RM4-5	APC
IgG1	BD Pharmingen	550874	X56	APC
IgM	BD Pharmingen	550676	II/41	APC
MAC1	BD Pharmingen	553312	M1/70	APC
CD25	BD Pharmingen	561038	PC61	APC-Cy7
CD19	BD Pharmingen	553785	1D3	FITC
CD21	BD Pharmingen	553818	7G6	FITC
Ig,k	BD Pharmingen	550003	187.1	FITC
CD93	BD Pharmingen	559156	AA4.1	FITC
Annexin V	BD Pharmingen	556419	na	FITC
CD138	BD Pharmingen	553714	281-2	PE
CD23	BD Pharmingen	553139	B3B4	PE
CD95	BD Pharmingen	554258	Jo2	PE
IgD	BD Pharmingen	558597	11-26c.2a	PE
B220	BD Pharmingen	553090	RA3-6B2	PE
CD43	BD Pharmingen	553271	S7	PE
CD5	BD Pharmingen	553023	53-7.3	PE
CD8	BD Pharmingen	553032	53-6.7	PE
CD95	BD Pharmingen	557653	Jo2	PE-Cy7
B220	BD Pharmingen	553093	RA3-6B2	PerCP
CD86	eBioscience	17-0862	GL1	APC
CD38	ebioscience	11-0381	90	FITC
CD93	ebioscience	25-5892	AA4.1	PE-Cy7
CXCR4	eBioscience	46-9991	2B11	PerCP-eFluor 710
IgD	Miltenyi biotec	130-103-005	11-26c.2a	VioGreen
PNA	Vector	FL-1071	na	FITC

na, not applicable.